Reviewed Preprint
v1 • March 31, 2026
Not revised

Reviewed Preprint
v2 • June 8, 2026
Revised by authors

For correspondence:
sjyou@fafu.edu.cn

† These authors contributed equally to this work

Competing interests: No competing interests declared

Funding: See page 32

Reviewing editor: Ariel Chipman, The Hebrew University of Jerusalem, Israel

Experimental evolution to thermal stress indicates climate resilience in a cosmopolitan arthropod

Gaoke Lei[1,2,3,†], Huiling Zhou[1,2,3,†], Zongyao Ma[1,2,3], Yating Duan[1,2,3], Yanting Chen[1], Fengluan Yao[1], Minsheng You[1,2,3], Liette Vasseur[1,2,4], Geoff M Gurr[1,2,5], Shijun You[1,2,3]

[1]State Key Laboratory of Agriculture and Forestry Biosecurity, Institute of Applied Ecology, Fujian Agriculture and Forestry University; Institute of Plant Protection, Fujian Academy of Agricultural Sciences, Fuzhou, China • [2]International Joint Research Laboratory of Ecological Pest Control, Ministry of Education, Fujian Agriculture and Forestry University, Fuzhou, China • [3]Ministerial and Provincial Joint Innovation Centre for Safety Production of Cross-Strait Crops, Fujian Agriculture and Forestry University, Fuzhou, China • [4]Department of Biological Sciences, Brock University, St. Catharines, Canada • [5]Gulbali Institute, Charles Sturt University, Orange, Australia

eLife Assessment

This **important** study deepens our understanding of how populations of a given species may diverge in their molecular and physiological patterns as a result of adaptation to different thermal regimes. By approaching this question from multiple directions, the authors provide **convincing** evidence for adaptive changes in three strains of the diamondback moth after only three years of experimental evolution. This work will be of interest to anyone working on the response of pest species to environmental change and to workers on adaptive evolution in general.

https://doi.org/10.7554/eLife.110352.2.sa3

Abstract

Adaptive evolution enables species to survive and thrive under changing environmental conditions. In the face of accelerating global climate change, thermal stress represents a major challenge to the persistence of terrestrial arthropods. Understanding the genetic mechanisms underlying thermal adaptation is therefore critical for predicting species' evolutionary potential and future success. Here, we combine experimental evolution, phenotypic assays, and multi-omics analyses to investigate the adaptive responses of the diamondback moth (*Plutella xylostella*), a globally destructive pest of cruciferous crops, to contrasting thermal environments. Populations evolved under hot (32°C/27°C) and cold (15°C/10°C) regimes exhibited distinct life history and fitness traits relative to those maintained under favorable conditions (26°C). The hot strain showed accelerated development, higher fecundity, and increased survival under extreme heat, while the cold strain exhibited lower supercooling and freezing points, indicating enhanced cold hardiness. Integrated transcriptomic and metabolomic analyses revealed extensive transcriptional reprogramming and convergent metabolic adjustments, notably a reduction in lipid metabolism to conserve energy under thermal stress. Crucially, non-synonymous mutations in *PxSODC* enhance superoxide scavenging efficiency, enabling effective oxidative stress management at lower gene expression levels. Furthermore, we identified epigenetic regulation via DNA methylation as a key mediator of this thermal tolerance. Together, these coordinated mutational, epigenetic, and metabolic insights highlight this arthropod's capacity for global dispersal and likely persistence under climate change, establishing a framework for understanding equivalent effects in other species.

Introduction

Human-induced climate change, particularly the continued change in temperature and precipitation patterns (IPCC, 2023), is altering the geographical distribution of insect pests, allowing those previously confined by temperature barriers to spread to new areas and posing growing threats to crop production and food security (Deutsch et al., 2008; Outhwaite et al., 2022; Lawlor et al., 2024). Such range expansion requires adaptation not only to warmer conditions in existing habitats but also to cold extremes encountered during colonization of higher latitudes or elevations (Harvey et al., 2020). As poikilothermic organisms with high surface area to volume ratios, insects are particularly responsive to temperature change (Wang et al., 2022), and species with higher genetic diversity and adaptive potential may be better equipped to cope with novel thermal environments, giving them an advantage in expanding into new habitats.

Adaptive evolution is a crucial mechanism for insect pests to expand their geographical ranges under climate change (McCulloch and Waters, 2022; Burc et al., 2025). Understanding the genetic basis of thermal adaptation is therefore essential for predicting how and ultimately where pest species will colonize new regions as temperature barriers shift (Gibert et al., 2019). Genetic mutations, particularly non-synonymous mutations, can alter protein structure or function and increase thermal tolerance (Belfield et al., 2018). For example, nonsynonymous mutations in the *AcVIAAT* gene of the eastern honeybee, *Apis cerana* (e.g., P42L substitution), are associated with enhanced thermal adaptation (Li et al., 2024c). and the alpine ground beetle, *Nebria vandykei*, achieve survival in extreme thermal environments through adaptive selection of mutations in key genes (*TREH*, *EIF3A*, *LRPPRC*, etc.) coupled with immediate responses from heat shock proteins (Schoville et al., 2024). Although significant progress has been made in identifying such mutations in non-model organisms, we do not yet know how long-term thermal selection drives coordinated changes across gene function, metabolic networks, and life history traits to enable thermal adaptation and range expansion in pest species.

The diamondback moth (DBM), *Plutella xylostella* (Lepidoptera: Plutellidae), is a globally distributed pest of cruciferous crops thriving across a wide range of climatic conditions (Furlong et al., 2013). Genome-wide SNP analysis of field populations from 114 locations revealed climate-adaptive genetic variability, suggesting that *P. xylostella* can tolerate projected future climates in most regions (Chen et al., 2021). These features, together with the availability of complete genome sequences and extensive SNP datasets (You et al., 2013; You et al., 2020), make it an ideal model for studying the genetic basis of thermal adaptation through integrated multi-omics approaches. Here, we investigate the mechanisms of *P. xylostella*'s genetic adaptation and evolutionary responses to different thermal environments. Specifically, we employ thermal regime patterns of 12h/12h in hot (32°C/27°C) or cold (15°C/10°C) environments over the course of three years (~75 and ~15 generations for the hot and cold strains, respectively), compared to the favorable constant condition at 26°C, to investigate the adaptive evolution of *P. xylostella* in climate-controlled chambers.

Age-stage, two sex life tables (a demographic method that simultaneously incorporates age, developmental stage, and both sexes; Chi, 1988) of *P. xylostella* measured the life history variation of the three *P. xylostella* strains evolved in the favorable (ancestral), hot and cold environments. Using metabolomic and transcriptomic analyses, we identified the key genes that could facilitate the adaptation of *P. xylostella* to thermal extremes. Our results showed that a large number of differentially expressed genes and metabolites were produced in populations adapted to high and low temperatures through multi-generational selection. We find the mutant of a key gene, *PxSODC*, which can alter the superoxide dismutase activity and increase the ability to scavenge superoxide anions. Since extreme temperatures elevate intracellular reactive oxygen species that damage cellular structures, this enhanced scavenging capacity helps maintain cellular homeostasis, thereby significantly affecting the adaptability under high and low temperature environments. CRISPR-Cas9 was used to functionally validate the role of *PxSODC* in facilitating adaptive evolution and influencing regulatory networks. These findings demonstrate that long-term thermal selection drives coordinated transcriptomic, metabolic, and life history divergence

in *P. xylostella*, and identify non-synonymous mutations in *PxSODC* that enhance superoxide scavenging efficiency as a key genetic mechanism underlying thermal adaptation, providing a framework for predicting its population dynamics under global climate change.

Results

Life history trait divergence among temperature-adapted strains

Following three years of evolution under contrasting thermal regimes (~75 and ~15 generations for the hot and cold strains, respectively), the hot strain (HS), cold strain (CS), and ancestral strain (AS) exhibited divergent life history traits. The hot strain exhibited an accelerated life cycle and increased fecundity, while the cold strain had extended male longevity. Specifically, both hot and cold strains had a significantly shorter preadult duration than the ancestral strain. The hot strain also had significantly shorter female longevity, and oviposition days, while the cold strain had a longer male longevity when compared to the ancestral strain (Supplementary File 1). The female fecundity, population intrinsic rate of increase (*r*) and finite rate of increase (λ) were all significantly higher in the hot strain than the cold strain which was not significantly different than the ancestral strain (Supplementary File 1). Detailed age-stage survival and fecundity curves are provided in Appendix 1.

To assess the evolved thermal tolerance of the temperature-adapted strains, we further examined the stage-specific survival rates of the hot and ancestral strains under extremely high temperatures, as well as the supercooling and freezing points of the cold and ancestral strains at pupae stage. The survival rates of eggs, 3rd-instar larvae and adults in the hot strain were higher than those of the ancestral strain at 42°C (e.g., 3rd-instar larvae at 120 min: HS 26.67% ± 3.57% vs. AS 13.33% ± 2.47%), and the survival rate of pupae in the hot strain was higher than that in the ancestral strain at 43°C and 44°C (Figure 1A). The supercooling and freezing points of pupae in the cold strain (supercooling: -23.99 ± 0.18°C; freezing: -14.24 ± 0.61°C) were significantly lower than those in the ancestral strain (supercooling: -23.09 ± 0.26°C; freezing: -11.58 ± 0.52°C), with differences of 0.90°C and 2.66°C, respectively (Figure 1B). The variation in survival rates and the supercooling/freezing points at extreme temperatures suggest that the hot and cold strains of *P. xylostella* have undergone profound adaptive adjustments.

Omics-based evidence for adaptive evolution

Our previous studies have identified metabolites such as trehalose and very long chain fatty acids that play a role in adaptation of *P. xylostella* to both high and low temperatures (Zhou et al., 2022; Lei et al., 2023). We performed a broad analysis of targeted metabolites of 3rd-instar larvae of each strain using high-throughput UPLC-MS/MS. A total of 781 metabolites were identified, including 199 amino acids and their metabolites, 146 lipids, 90 organic acids and their derivatives, 78 nucleotides and their metabolites, 61 heterocyclic compounds, 45 benzene and substituted derivatives, 42 alcohols and amines, 37 carboxylic acids and derivatives, 21 coenzymes and vitamins, and 62 other metabolites (Figure 2A). Principal component analysis (PCA) and inter-sample correlation heat maps revealed significant metabolic changes in the 3rd-instar larvae from the ancestral strain to the hot and cold strains (Figure 2B; Figure 2–figure supplement 1A). These comprised 77 differential metabolites (34 up-regulated, 43 down-regulated compared to the ancestral strain) in the hot strain, and 37 differential metabolites (13 up-regulated, 24 down-regulated compared to the ancestral strain) in the cold strain (Figure 2C).

Compared to the ancestral strain, the common differential metabolites of the hot and cold strains included lipids, amino acids and their metabolites, organic acids and their derivatives, nucleotides and their metabolites, and benzene and substituted derivatives (Figure 2D; Figure 2–figure supplement 1B). Inter-replicate analysis of differential metabolites showed a low correlation between the ancestral strain and hot/cold strains, but a high correlation between the hot and cold strains (Figure 2–figure supplement 1C). Notably, 30 common metabolites were identified across the differential sets based on comparison of the hot/cold strains to the ancestral strain (Figure 2E). These metabolites, except for N1, N8-diacetylpiperidine, exhibited similar fold changes

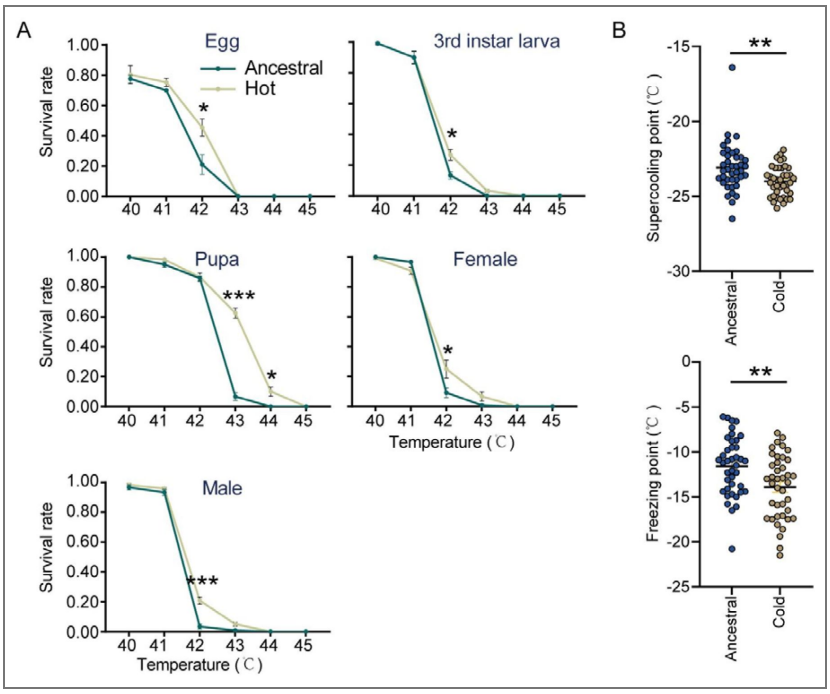

Figure 1. Evolved phenotypic changes in temperature-adapted strains.

(A) Stage-specific thermal tolerance responses (survival rates) of the ancestral and hot strains, with 20 individuals used in each of the six replicates for every treatment. (B) Supercooling and freezing points of pupae for the ancestral and cold strains, with 40 biologically independent samples used in each treatment. Data are presented as mean ± SEM. Statistical analyses are performed using t-tests with significant levels indicated by asterisks (*$p < 0.05$, **$p < 0.01$, ***$p < 0.001$).

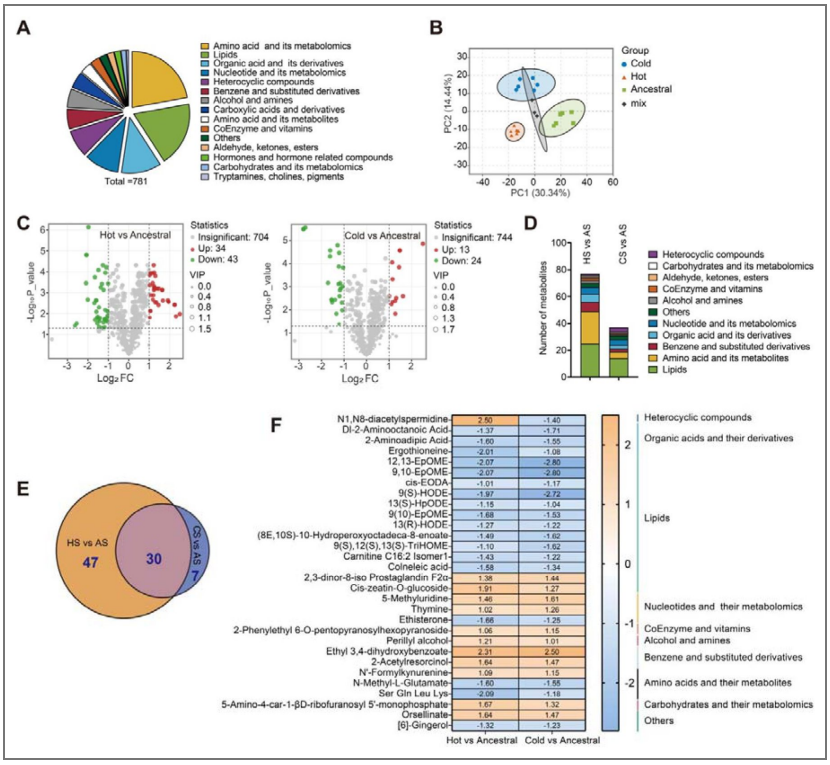

Figure 2. Metabolomic analysis of 3rd-instar larvae across ancestral, hot and cold strains (AS, HS and CS).

(A) Classification of metabolites, with a total of 781 metabolites being identified in different strains. (B) Principal component analysis (PCA) of the 781 metabolites across different strains. PC1 and PC2 represent the first and second principal components, respectively. (C) Volcano plot showing the down-regulated (green dots) and up-regulated (red dots) metabolites based on comparison between HS/CS and AS. (D) Classification of differential metabolites between HS/CS and AS. (E) Venn diagram showing the common and unique differential metabolites in HS and CS as compared to AS. (F) Fold changes and classifications of the common differential metabolites in HS and CS as compared to AS.

when comparing the hot/cold strains to the ancestral strain (Figure 2F). These results indicate that *P. xylostella* responds to different environmental stresses by regulating similar metabolic pathways. Further analysis revealed a reduction in most of the lipid metabolites in both HS and CS compared to AS (Figure 2F).

We then profiled and compared the transcriptomes of the three strains to identify the key genes involved in adaptation of *P. xylostella* to temperature extremes. This revealed significant variation in gene expression among strains (Figure 3A; Figure 3–figure supplement 1A), with 1364 (825 up-regulated, 539 down-regulated) and 2029 (1205 up-regulated, 824 down-regulated) genes differentially expressed in the hot and cold strains, compared to the ancestral strain (Figure 3B). Pearson correlation showed, in contrast to the metabolomics data, a lack of strong correlation between the differentially expressed genes of the hot/cold strains and the ancestral strain (Figure 3C), with 498 common differentially expressed genes (Figure 3D). However, KEGG analysis revealed that the differentially expressed genes between the hot/cold strains and the ancestral strain were enriched in a substantial overlap of similar pathways, such as transport and catabolism, signal transduction, and lipid metabolism (Figure 3E), indicating that while multiple genes are involved in the adaptation of *P. xylostella* to high and low temperatures, a relatively limited range of biological functions might be affected.

The gene expression-based clustering tree using a weighted gene co-expression network analysis (WGCNA) was divided into 29 modules as shown with alphanumeric identifiers (M1-M29) (Figure 4A; Figure 3–figure supplement 1B). Module M4 contained the most genes (3463), while module M29 contained the fewest (31) (Figure 4B). Selecting the common differential metabolites (30 in total) shared between the hot and cold strains as compared to the ancestral strain, we performed a correlation analysis with co-expressed networks and found that multiple modules, including modules M13, M19, and M24, showed strong correlations with shared differential metabolites. Module M13 was selected for further analysis as it had the highest number of significantly correlated metabolites (28 of 30) (Figure 4C; Figure 3–figure supplement 1C). Further analysis revealed that 79 genes within module M13 were differentially expressed in the hot and cold strains when compared with the ancestral strain (Figure 4D). These results suggest that genes in module M13 may be candidates involved in the adaptation of *P. xylostella* to extreme temperatures.

Genetic basis of temperature adaptation

To further elucidate the genetic basis of *P. xylostella* adaptation to hot and cold environments, from the 79 candidate genes identified above, we selected 15 that were annotated in the genome and had high expression levels (FPKM > 10) for further analysis (Figure 4D) and identified 11 genes being successfully amplified. Comparative results revealed eight genes with nonsynonymous mutations and one with a synonymous mutation in both the hot and cold strains (Supplementary File 2). Among these genes, we focused on the role of *Px04C00666* (*PxSODC*) in temperature adaptation of *P. xylostella* because the deletion of superoxide dismutase (SOD) genes can alter the response of insects to abiotic stresses including temperature (Bittner et al., 2019; Quan et al., 2024).

The NCBI database predicted that *PxSODC* contained three exons and two introns, with a conserved domain belonging to the copper-zinc superoxide dismutase superfamily (Figure 5–figure supplement 1A) which plays an antioxidative role in cellular defense systems, protecting cells from damage caused by reactive oxygen species (***Fridovich, 1995***). The open reading frame of *PxSODC* was 633 bp and encodes 210 amino acids. Expasy predicted that the molecular weight of the PxSODC protein was 22,168.24 Da, with the isoelectric point being 6.29. According to PSIPRED predictions, its secondary structure consisted of approximately 55.24% random coils, 16.19% alpha helices, and 28.57% extended strands (Figure 5–figure supplement 1B). Evolutionary analysis using a Maximum Likelihood approach showed *PxSODC* of *P. xylostella* clustered with that of other Lepidoptera insects such as *Operophtera brumata*, *Vanessa cardui*, and *Cydia fagiglandana*, indicating its conserved evolution within this taxonomic order (Figure 5–figure supplement 1C). The coding region of *PxSODC* in the hot and cold strains had 23 SNP sites, including 20

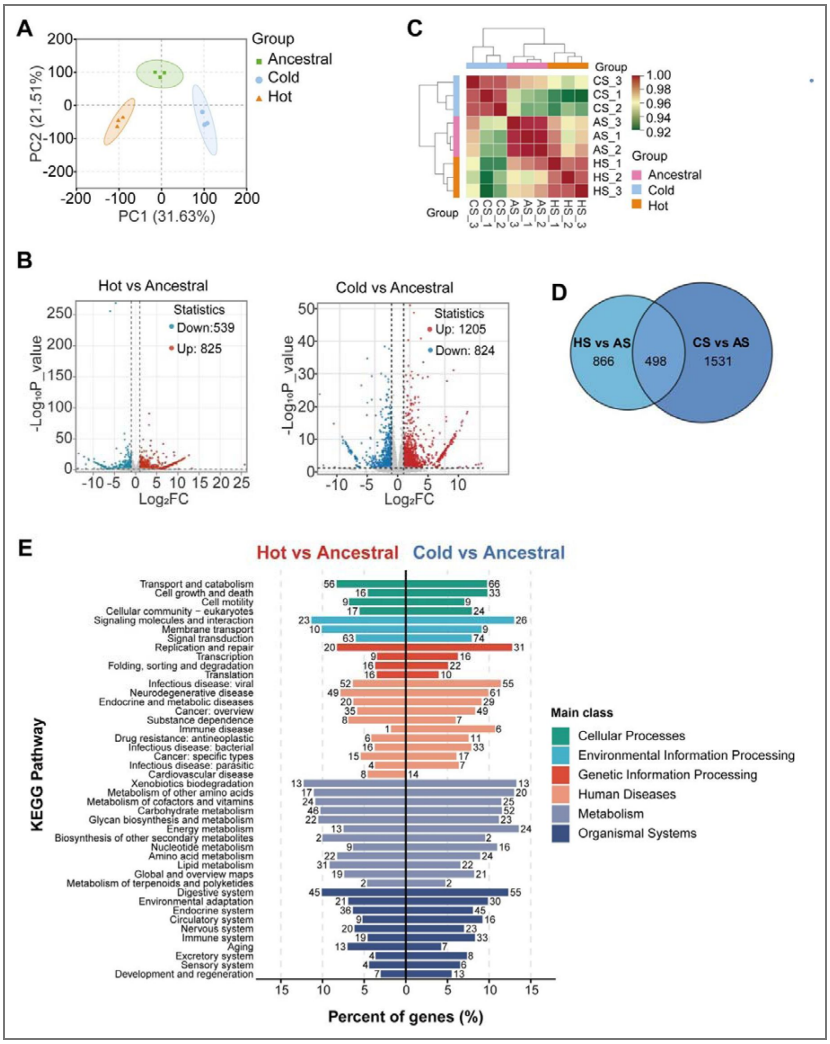

Figure 3. Transcriptomic analysis of the 3rd-instar larvae across the ancestral, hot and cold strains.

(A) Principal component analysis (PCA) of genes across different strains. PC1 and PC2 represent the first and second principal components, respectively. (B) Volcano plots of differential gene expression, showing significantly up-regulated (red dots) and down-regulated (green dots) genes between HS/CS and AS (FDR < 0.05, fold change > 2). (C) Cluster analysis of the transcriptome. The colors represent the Pearson correlation coefficients between samples, indicating transcriptomic similarity. (D) The number of common or unique differentially expressed genes between HS/CS and AS. (E) KEGG function classification of differentially expressed genes between HS/CS and AS.

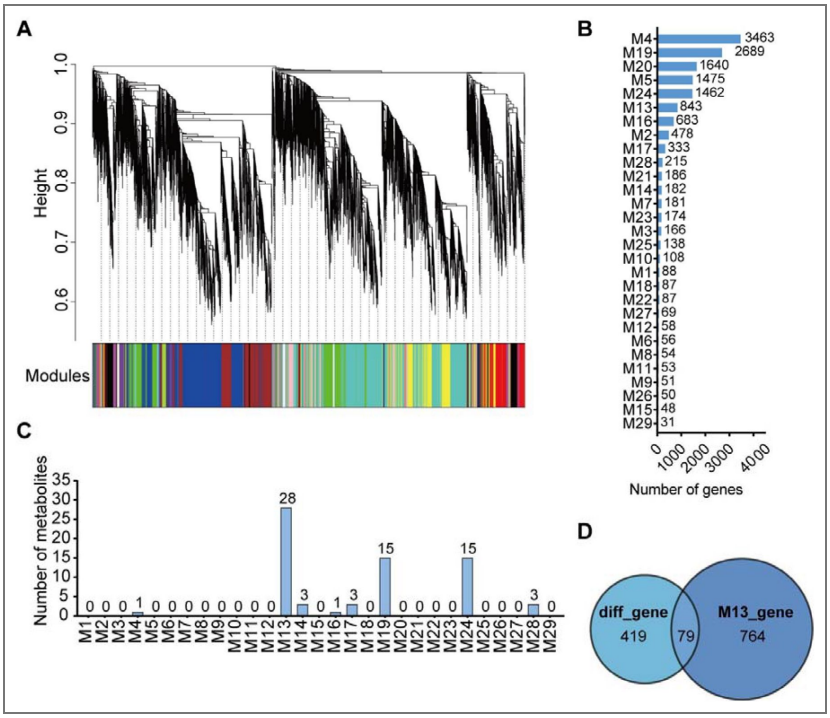

Figure 4. Weighted gene co-expression network analysis (WGCNA) of transcriptomes for the 3rd-instar larvae across the ancestral, hot and cold strains (HS, CS and AS) of *P. xylostella*.

(A) Hierarchical cluster tree illustrating 29 modules identified by WGCNA. (B) Numerical distribution of genes of different modules as identified by WGCNA clustering. (C) In WGCNA, module M13 shows the highest number of metabolites strongly correlated with genes. (D) Overlap of genes in module M13 from WGCNA with common differentially expressed genes between HS/CS and AS.

synonymous and three non-synonymous mutations (Leu9-Val9, Lys25-Gln25, Leu194-Met194) (Figure 5A-B). Leu9-Val9 and Leu194-Met194 mutations were involved in the substitution of hydrophobic amino acids. Based on sequencing of 10 individuals per strain, the Leu194-Met194 mutation was present at a frequency of 70% in HS, 90% in CS, and 30% in AS (Figure 5B). The expression of *PxSODC* at different developmental stages of the hot and cold strains was significantly lower than that of the ancestral strain (Figure 5–figure supplement 2A). After 2 h exposure of the 3rd-instar larvae to the stress of high (32°, 34°, 36°, 38° and 40°C) or low (12°, 10°, 8°, 6° and 4°C) temperature environments, the expression of *PxSODC* in the hot and cold strains was significantly lower than in the ancestral strain (Figure 5–figure supplement 2B-C). This suggests that the expression of the *PxSODC* gene is regulated by temperature triggers, and its altered function contributes to the temperature-adaptive evolution in *P. xylostella*.

To elucidate the structural mechanism by which these non-synonymous mutations enhance protein function under thermal stress, we performed 100 ns MD simulations on AlphaFold-generated models of the wild-type (WT) and mutant (MU) PxSODC at 15°C, 26°C (favorable baseline), and 32°C (Figure 5–figure supplement 3). RMSD analysis revealed that at the 26°C baseline, both WT and MU exhibited comparable structural stability (1.62 ± 0.21 vs. 1.59 ± 0.27) (Figure 5–figure supplement 3B). However, under heat stress (32°C), WT underwent severe conformational drift (RMSD surged to 2.49 ± 0.35, an increase of 0.87 from baseline), while MU remained remarkably stable (1.66 ± 0.26, an increase of only 0.07) (Figure 5–figure supplement 3C). SASA analysis showed that MU possessed an inherently more compact structure than WT, with lower values at both 15°C (118.39 ± 7.57 vs. 127.29 ± 6.12 nm^2) and 26°C (113.82 ± 7.40 vs. 125.61 ± 6.76 nm^2), indicating optimized hydrophobic core packing (Figure 5–figure supplement 3D). Analysis of intramolecular hydrogen bonds further revealed that the MU network exhibited dual stress resistance: under cold stress (15°C), MU actively increased hydrogen bonds from its 26°C baseline (113 → 119), demonstrating a compensatory response, while WT suffered bond loss (117 → 112); under heat stress (32°C), MU fully maintained its hydrogen bond count (113 → 113), whereas WT showed a slight decrease (117 → 116) (Figure 5–figure supplement 3E). Collectively, these simulations demonstrate that the non-synonymous mutations confer enhanced global structural rigidity and dual-directional thermal resilience to PxSODC through a more compact hydrophobic core and a more resilient intramolecular hydrogen bond network, providing a direct structural basis for its increased catalytic efficiency at lower expression levels.

The above analyses revealed naturally occurring non-synonymous mutations in *PxSODC* that are enriched in the hot and cold strains. To directly test whether *PxSODC* is functionally required for thermal adaptation, we generated loss-of-function mutants by disrupting *PxSODC* in the ancestral strain using CRISPR/Cas9-mediated mutagenesis. Of 162 eggs treated with CRISPR/Cas9, 75 successfully developed into adults. We confirmed three mutant strains in the G0 generation of *P. xylostella*: +1 bp (SODC-MU1), +2 bp (SODC-MU2) and -1 bp (SODC-MU3). Self-crossing continued, and three types of homozygous mutation were obtained in the G5 generation (Figure 5–figure supplement 4). Life table analysis showed that the three SODC-MU strains had prolonged development, lower survival rates, and reduced fecundity and population fitness compared to the ancestral strain, particularly under hot/cold environments (Appendix 2; Figure 5–figure supplement 5; Supplementary File 3-5).

We then assessed the stage-specific survival of the ancestral strain and all three SODC-MU mutant strains (SODC-MU1, SODC-MU2 and SODC-MU3) under extreme heat stress to determine whether *PxSODC* loss consistently impairs thermal tolerance. At 42°C, the survival rates of eggs, 3rd-instar larvae, female adults and male adults of the mutant strains were significantly lower from those of the ancestral strain at several time points (Figure 5C). However, survival rates of the mutant pupae exposed to the high temperature (43°C) were not significantly different from those of the ancestral strain at different time points (Figure 5C). The pupal stage appeared more tolerant to high temperature than other life stages, as the *PxSODC* knockout did not significantly reduce pupal survival at 43°C while it significantly reduced survival of eggs, larvae, and adults at 42°C (Figure 5C). This may be due to pupal-specific heat resistance mechanisms, such as protective chrysalis and U-shaped metabolism (Kaiser et al., 2010; Barros-Cordeiro et al., 2014). In addition,

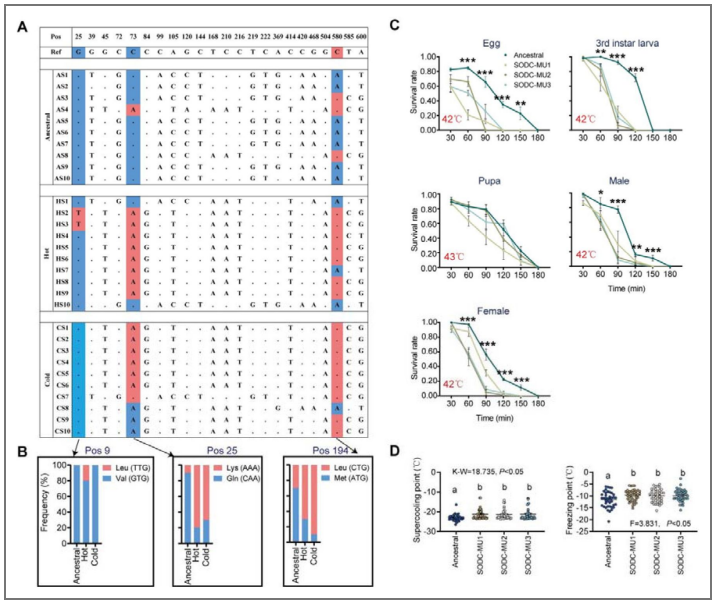

Figure 5. Role of *PxSODC* in temperature adaptation of *P. xylostella*.

(A) Allele frequencies of SNPs in the *PxSODC* gene amplified by PCR from the ancestral, hot and cold strains (AS, HS and CS). The analysis involves ten 4th-instar larvae from each of the strains; the dot (·) indicates identity with the reference base. (B) Frequency of amino acid translations from non-synonymous codon mutations in the *PxSODC* gene in different strains. (C) Stage-specific survival rates of the ancestral and mutant strains (AS, SODC-MU1, SODC-MU2 and SODC-MU3) under extreme heat conditions. (D) Supercooling and freezing points of the pupae from different strains (AS, SODC-MU1, SODC-MU2 and SODC-MU3). Data are presented as mean±SEM, one-way ANOVA with Tukey's test was used for comparison.Six biologically independent samples were used in (C) and significant levels between groups with the same stress duration are indicated by asterisks (*p < 0.05, **p < 0.01, ***p < 0.001). A total of 40 biologically independent samples were used in (D) and statistical significance is indicated by different letters (p < 0.05).

supercooling and freezing points of the mutant strains (MU1: -21.32±0.41 and -9.75±0.38; MU2: -21.50±0.38 and -9.93±0.43; MU3: -21.23±0.48 and -9.94±0.41) were significantly higher than those of the ancestral strain (-23.09±0.26 and -11.58±0.52) at pupal stage (Figure 5D), indicating a key role of the *PxSODC* gene in the adaptability and tolerance of *P. xylostella* to extreme temperatures.

To further investigate the effect of *PxSODC* gene mutations on the temperature adaptability of *P. xylostella*, we identified five genes from the same SOD family in transcriptomes of the 3rd-instar larvae from the three tested strains. We found that *Px04C00505* and *Px13C00423* showed SNP mutations in the hot and cold strains, whereas *Px20C00248*, *Px15C00224* and *Px15C00223* were not mutated (Supplementary File 6). Further comparison of gene expressions across different strains revealed that, relative to the ancestral strain, the expression levels of *PxSODC*, *Px04C00505*, and *Px13C00423* were significantly reduced in the hot and cold strains, while the remaining genes maintained stable or increased expression levels (Figure 6A). Concurrently, SOD activity decreased in the hot and cold strains, along with a reduction in O_2^- levels (Figure 6B-C). When SOD expression and activity, as well as O_2^- levels, were compared under different temperature conditions between the ancestral and hot/cold strains, similar patterns were observed (Figure 6D-F). These results suggest that non-synonymous mutations in the hot and cold strains may alter SOD protein conformation, increasing catalytic efficiency per molecule and enabling effective O^- scavenging at lower expression levels. This energy-efficient strategy is beneficial under thermal stress, where conserving metabolic resources for development and reproduction is critical for survival. Compared to the ancestral strain, expression of the mutated *SODC* genes (*Px04C00505* and *Px13C00423*) was increased in the male adults in SODC-MU1 and SODC-MU2. The expression levels of the non-mutated genes *Px20C00248*, *Px15C00224* and *Px15C00223* were also increased (Figure 6G). Further, SOD activity decreased, while O_2^-levels increased in the two mutant strains (Figure 6H-I), which were unable to fully compensate for the effects caused by the deletion of the *PxSODC* gene, implying that the SOD protein encoded by *PxSODC* plays a crucial role in O_2^- scavenging.

PxSODC-allied metabolic networks

Untargeted metabolomic analysis of the ancestral and SODC-MU strains across developmental stages revealed broad metabolic adjustments involving lipids, nucleotides, carbohydrates, and amino acids following *PxSODC* deletion (Appendix 3; Figure 7-figure supplement 1 and 2). In the metabolome, the abundance of three metabolites, namely 5-hydroxymethyluracil, 2-methylcitric acid, and 5'-deoxyadenosine, differed between the mutant strains (SODC-MU1 and SODC-MU2) and the ancestral strain across all developmental stages (Figure 7A). With the exception of 5'-deoxyadenosine, which was significantly higher in the 3rd-instar larvae, these three metabolites were significantly lower in other developmental stages of the mutant strains (Figure 7B). This suggested a possible direct association with *PxSODC*, and may represent a key biological regulatory response in *P. xylostella*'s adaptation to different environmental conditions. Importantly, this specific metabolic signature provided a compelling, data-driven hypothesis linking *PxSODC*-mediated oxidative stress management directly to epigenetic regulation: 5-hydroxymethyluracil is directly involved in dynamic DNA demethylation, and 5'-deoxyadenosine is a precursor to S-adenosylmethionine, the primary methyl donor for DNA methylation (Bhutani et al., 2011; McKean et al., 2019). Their consistent alteration in the SODC-MU strains suggested a potential link between *PxSODC* and DNA methylation. To test this hypothesis, we measured the expression levels and enzymatic activities of DNA methyltransferase 1 (*PxDnmt1*) in the 3rd-instar larvae of different strains. The results showed that both the expression and enzymatic activity of *PxDnmt1* were significantly reduced in the hot and cold strains compared to the ancestral strain (Figure 7C-D). Using RNA interference (RNAi) technology, we specifically silenced the expression of *PxDnmt1* in the ancestral strain of *P. xylostella* (Figure 7E) and observed significantly reduced levels of 5-methylcytosine (5-mC, a marker of DNA methylation) in both pupae and female adults (Figure 7F) (Ni et al., 2023). Further, we found that silencing of *PxDnmt1* could significantly decrease the critical thermal maximum (CTmax) of female adults and increase the supercooling and freezing points of pupae (Figure 7G-H). These results suggest that DNA methylation may

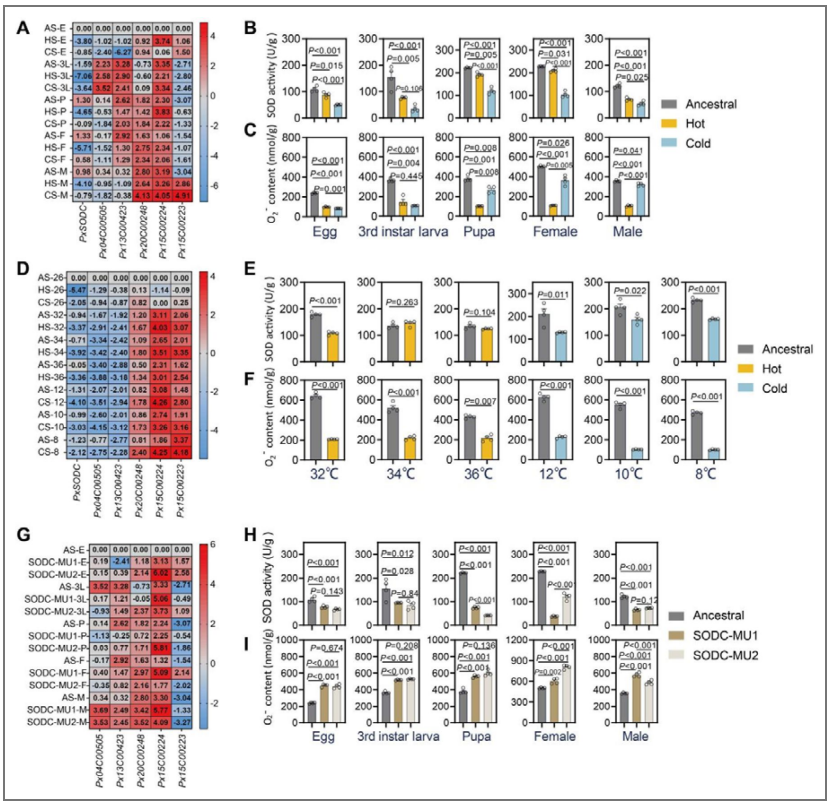

Figure 6. SOD expression and activity and superoxide anion (O_2^-) levels across developmental stages and temperature environments in different strains of *P. xylostella*.

(A) Expression levels of the *SOD* genes at different developmental stages of AS, HS, and CS in the favorable temperature environment (26°C). (B) SOD enzyme activity at different developmental stages of the ancestral, hot and cold strains (AS, HS, and CS) in the favorable temperature environment. (C) O^- levels at different developmental stages of AS, HS, and CS in the favorable temperature environment. (D) Expression levels of the genes from the *SOD* family in the 3rd-instar larvae of AS, HS, and CS in the hot (32°C, 34°C, 36°C) and cold (12°C, 10°C, 8°C) environments. (E) SOD enzyme activity in the 3rd-instar larvae of AS, HS, and CS in the extreme temperature environments. (F) O_2^- levels in the 3rd-instar larvae of AS, HS, and CS in the hot and cold environments. (G) Expression levels of *SOD* family (excluding the *PxSODC* gene) at different developmental stages of the ancestral and SODC-MU strains in the favorable temperature environment. (H) SOD enzyme activity at different developmental stages of the ancestral and SODC-MU strains in the favorable temperature environment. (I) O^- levels at different developmental stages of the ancestral and SODC-MU strains in the favorable temperature environment. n = 3 biologically independent samples in (A), (D), (G); within each of the boxes, the numerical value represents log_2-fold change of the gene expression level in the treated samples with respect to the control. n = 4 biologically independent samples in (B), (C), (E), (F), (H), with data being presented as mean±SEM. One-way ANOVA with Tukey's test was used for comparison in (A), (B), (C) and (G), (H), (I) ($p < 0.05$). t-test was used for comparison in (D), (E), (F) ($p < 0.05$).

play a role in the thermal tolerance of *P. xylostella*, though further work is needed to establish a direct mechanistic link between *PxSODC*, methylation-related metabolites, and epigenetic regulation of thermal adaptation.

Discussion

Insects are valuable bio-indicators of the effects of climate change via their phenology, distribution, population dynamics responses (Bale et al., 2002; Halsch et al., 2021). The present study demonstrates that *P. xylostella* can undergo rapid genetic adaptation to thermal extremes, providing mechanistic insights into how this globally invasive pest may expand its range under climate change through coordinated transcriptomic, metabolomic, and life history changes. By conducting the life history trait, demography, and fitness assessment of the ancestral, hot and cold strains of *P. xylostella*, we observed that the hot and cold strains had evolved significant genetic differences from the ancestral strain in multiple traits related to thermal tolerance and fitness. In the context of global warming, *P. xylostella* may evolve greater flexibility across its range and ecological niche leading the hot-evolved populations to be able to persist in regions with increased temperatures due to climate change (Chen et al., 2021). With climate change, cold-adapted *P. xylostella* may be favored during episodes of late frost in the spring or early frost in the autumn in temperate regions. The lower supercooling and freezing points of the cold strain pupae facilitate the survival of insects in cold climates, extending their ecological adaptability to low-temperature environments (Block, 1997). The demonstrated capacity of *P. xylostella* to adapt to extreme thermal conditions of both forms implies that *P. xylostella* may survive under a broader range of climatic conditions, posing new challenges for the management and control of this worldwide pest.

Our findings reveal a significant metabolic adjustment in *P. xylostella* during its adaptive evolution to both high and low temperatures. The convergent reduction of lipid-related metabolites such as octadecenoic acid, epoxystearic acid, and carnitine in both the hot and cold strains (Figure 2F) suggests a shared metabolic adjustment during thermal adaptation. Lipids play a key role in energy storage and membrane stability in insects, and downregulation of lipid metabolism may enable *P. xylostella* to conserve metabolic resources and reallocate energy toward development and reproduction (Rommelaere et al., 2019; Mallard et al., 2018). As a key mediator of fatty acid transport and energy metabolism, the reduction in carnitine levels may further reflect this energy reallocation strategy (Bremer, 1983).

Although gene expression between the hot and cold strains does not show a strong correlation, KEGG analysis indicates that differentially expressed genes in both adapted strains share similarly enriched core pathways (Figure 3E). Notably, the convergent reduction in lipid metabolism represents a shared energy reallocation strategy. Freeing up resources to fuel the accelerated development, higher fecundity, and extreme-heat survival in the hot strain, while facilitating the extended male longevity and lower supercooling and freezing points required in the cold strain (Tigano et al., 2020; Sherpa et al., 2022; Li et al., 2024a). Relative to the ancestral strain, the cold strain exhibited more differentially expressed genes (2029 *vs.* 1364) but fewer differential metabolites (37 *vs.* 77) than the hot strain. This pattern contrasts with findings in *Drosophila*, where thermal adaptation produced a simpler transcriptomic (Mallard et al., 2018). This divergence in omics profiles strictly aligns with their distinct physiological requirements. The cold-adapted strain relies on broader transcriptional reprogramming to structurally maintain basic cellular homeostasis and sustain cold hardiness over its prolonged lifespan, whereas the hot-adapted strain utilizes targeted gene expression changes combined with broader metabolic rewiring to actively sustain rapid energy turnover and its accelerated life cycle.

Mutations in these genes during adaptive evolution in response of thermal adaptation can lead to novel phenotypic traits, such as changes in the life history and population fitness of insects (Gibson et al., 2019). The *PxSODC* gene encodes a superoxide dismutase (SOD) that scavenges superoxide anions in cells, maintaining redox balance and protecting cellular structures (Sheng et al., 2014). Under extreme temperatures, insects can adjust their survival strategy, allocating more energy to maintain fundamental life functions (Hoffmann and Sgro, 2011). Here, the

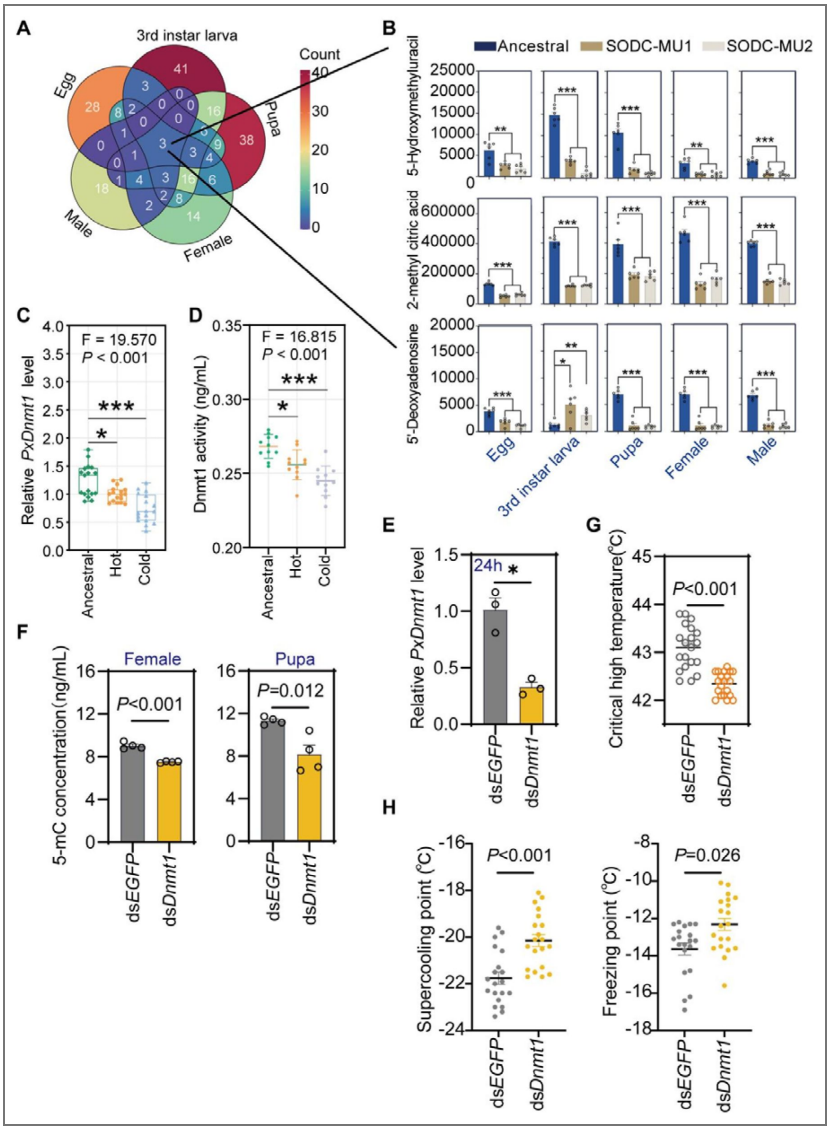

Figure 7. Comparison of metabolites and DNA methylation across different strains of *P. xylostella*.

(A) A Venn diagram showing the metabolites that are consistently different between the ancestral and mutant strains across different developmental stages. (B) Three metabolites with persistent discrepancy across different developmental stages in the ancestral and mutant and strains. (C) Expression level of the DNA methyltransferase 1 gene (*PxDnmt1*) in the ancestral, hot and cold strains. *n* = 17 biologically independent samples. (D) DNA methyltransferase activity in the ancestral, hot and cold strains. *n* = 12 biologically independent samples. Data are presented as mean±SEM, one-way ANOVA with Tukey's test was used for comparison in (C), (D) ($p < 0.05$). (E) Injection of ds*Dnmt1* significantly reduced the expression level of *PxDnmt1* in the ancestral strain of *P. xylostella*. *n* = 3 biologically independent samples. (F) Silencing of *PxDnmt1* decreased 5-methylcytosine (5-mC) content in the female adults and pupae of *P. xylostella*. *n* = 4 biologically independent samples. (G) Female adults with silenced *PxDnmt1* exhibited a significantly decreased critical thermal maximum (CTMax). *n* = 20 biologically independent samples. (H) Pupae with silenced *PxDnmt1* displayed elevated supercooling and freezing points. *n* = 40 biologically independent samples. Data are presented as mean±SEM, unpaired t-test was used for comparison in (E), (F), (G), (H) ($p < 0.05$).

deletion of the *PxSODC* gene led to reduced SOD enzyme activity and increased O_2^- levels, reducing the tolerance of *P. xylostella* to extreme temperatures. These findings provide novel insights into how genetic variation translates into phenotypic variation (You et al., 2024), and the ways in which *P. xylostella* responds – and has responded – to a changing climate (Chen et al., 2021).

Our molecular dynamics simulations provide direct structural evidence that the non-synonymous mutations enhance *PxSODC* protein thermostability (Figure 5–figure supplement 3). Specifically, the mutant protein maintained structural integrity under both heat and cold stress through a more compact hydrophobic core and a more resilient hydrogen bond network. This enhanced dual-directional thermostability likely increases catalytic efficiency per molecule, enabling effective superoxide scavenging at the lower expression levels observed in the evolved strains and reducing the energetic cost of enzyme production, consistent with previous findings that specific structural mutations can directly increase SOD enzyme activity (Sheng et al., 2013). After long-term adaptation, insects may acquire the ability to maintain cellular homeostasis in new thermal environments by reducing basal metabolism and allocating more energy to development and reproduction (Mallard et al., 2018). At 34°C and 36°C, the trends in SOD enzyme activity and *PxSODC* gene expression differ between different temperature-evolved strains, suggesting the involvement of additional genes in the regulation of SOD enzyme activity. This hypothesis is supported by our transcriptomic analysis which identified additional *SOD* genes (Supplementary File 5).

In the SODC gene family, two *SOD* genes (*Px04C00505* and *Px13C00423*) underwent non-synonymous mutations and showed reduced expression in the hot and cold strains at different developmental stages, while the expression of three *SOD* genes without mutations remained relatively stable or increased at most developmental stages. The evolution of protein functions is driven by mutations, which in some cases can switch directly from one function to another through single amino acid changes (Nobeli et al., 2009; Patsch et al., 2024). Under extreme temperatures, the expression of these genes in the 3rd-instar *P. xylostella* larvae of the hot and cold strains trends to be similar to those of the ancestral strain. This indicates that adverse environmental conditions increase intracellular oxidative stress, which requires regulation of SOD expression and enzyme activity to scavenge superoxide anions (Islam et al., 2022). Maintaining high levels of SOD enzyme activity requires additional energy, placing a strain on cellular energy metabolism and resource allocation (Emre et al., 2013). *SOD* genes with non-synonymous mutations, like *PxSODC*, can lead to the change in protein structure or function, affecting enzyme activity and allowing for faster O_2^- scavenging at lower transcript levels, reducing resource requirements. The three unmutated *SOD* genes, if mutated, might adversely affect the moth or have other functions, such as involvement in cellular signaling pathways (Mondola et al., 2016).

Metabolomic analysis of different developmental stages in the ancestral and mutant strains revealed that after the loss of *PxSODC* gene, the metabolism of *P. xylostella* underwent temperature-adaptive adjustments involving lipids, nucleotides, carbohydrates, coenzymes and vitamins, and amino acids. This study also showed that DNA methylation plays a key role in the temperature adaptation of *P. xylostella*. While DNA methylation may be associated with gene activation, its main function remains the inhibition of gene expression (Stroud et al., 2015; Wang et al., 2018). Transcriptomic analysis also showed that more genes were up-regulated in the hot and cold strains compared to the ancestral strain, highlighting the role of DNA methylation in regulating gene expression to help *P. xylostella* maintain physiological functions and survive. In addition to directly regulating the expression of temperature responsive genes, epigenetic effects can also indirectly affect the response of insects to temperature challenges (Reynolds, 2017). By adding the molecular data of epigenetic markers, underlying mechanisms on the adaptive adaptation can be more easily elucidated. Therefore, further work is required to better understand the impact of non-genetic effects on adaptation to future climates including how they interact with genetic adaptive capacity. While our experimental evolution approach successfully uncovered potential genetic mechanisms of thermal adaptation, its ecological relevance warrants consideration. Exposing the insects to extreme 12 h thermal bounds was necessary to impose strong directional selection and observe adaptive evolution over a relatively short timeframe (~3

years) in the laboratory. However, we acknowledge that comparing fluctuating stressful environments to a constant favorable environment (26°C) may conflate adaptation to absolute temperature extremes with adaptation to thermal fluctuation itself. Future field-based studies across natural gradients, or using fluctuating optimal control regimes, will be valuable to validate the ecological impact of these mutational and epigenetic pathways in wild habitats.

This study elucidates the molecular mechanisms underlying adaptation of *Plutella xylostella* to both high- and low-temperature environments and functionally validates differentially expressed genes identified in ancestral, hot-evolved, and cold-evolved strains. Nevertheless, thermal adaptation in arthropods may engage distinct, temperature-specific biological pathways; accordingly, future work will prioritize the characterization of strain-specific differentially expressed genes. Beyond functional validation of the canonical stress-associated gene *PxSODC*, additional genes harboring nonsynonymous mutations warrant detailed investigation to clarify their roles within the broader regulatory network. Importantly, our findings also underscore a critical role for DNA methylation in thermal adaptation in *P. xylostella*. More broadly, future research should integrate genetic, epigenetic, and metabolic approaches across diverse taxa to determine whether adaptive mechanisms such as SOD-mediated oxidative stress regulation and DNA methylation represent general strategies by which arthropod pests adapt to novel thermal environments and expand their ranges under climate change.

Materials and methods

Insects

The founding population of *P. xylostella* was established from field-collected larvae on cabbage (*Brassica oleracea* var. *capitata*) in organic farms in Fuzhou, Fujian Province, China (26°05'N, 119°18'E) in July 2012. Fuzhou experiences a subtropical monsoon climate, where summer high temperatures exceed 32°C and winter lows can drop below 10°C, making our experimental selection temperatures ecologically relevant extremes for this population. The collection site was confirmed through farmer interviews and local agricultural records to have no history of insecticide application for at least five years. Approximately 300-500 larvae were collected from multiple host plants distributed across a 2-hectare area to maximize genetic diversity and minimize founder effects. The field-collected population was reared in the laboratory under controlled conditions of 26°C and 60% relative humidity with a 12-h light/12-h dark cycle, without exposure to insecticides. This setup was referred to as the favorable temperature environment based on a previous study on the relationship between temperature and the *P. xylostella* development (Liu et al., 2002). Population size was maintained at >500 individuals per generation to minimize inbreeding and genetic drift. This laboratory-acclimated population was designated as the ancestral strain and served as the baseline for all subsequent experiments. Eggs and larvae were reared in sterile plastic disposable Petri dishes (90 mm) with an artificial diet containing 68 g yeast powder, 20.4 g agar, 127.5 g raw wheat germ, 3.4 g potassium sorbate, 3.4 g methyl paraben, 34 g sucrose, 10.2 g powder of radish seed, 1.7 g vitamin premix, 3.4 g ascorbic acid, 3.4 mL cola oil, 0.34 mL linoleic acid and 850 mL water The adults were allowed to mate and lay eggs in disposable paper cups, and were fed with a 10% honey solution.

The previous study on the relationship between temperature and developmental rate shows that *P. xylostella* can survive and develop at the temperatures 32°C at the maximum, 26°C as the optimum, and 10°C for the minimum (Liu et al., 2002). To generate thermally adapted populations, we established 18 replicate populations from the ancestral strain and randomly assigned them to three thermal regimes: (1) a hot-evolved treatment with cycling temperatures of 32°C/27°C (12 h light/12 h dark), (2) a cold-evolved treatment with cycling temperatures of 15°C/10°C (12 h light/12 h dark), and (3) a control treatment maintained at constant 26°C. The hot and cold regimes used cycling temperatures to simulate diurnal fluctuations experienced in natural environments, while the control was kept at the constant optimal developmental temperature for *P. xylostella* (Liu et al., 2002). All other environmental conditions (humidity,

Reagent type (species) or resource	Designation	Source or reference	Identifiers	Additional information
Strain, strain background (*Plutella xylostella*)	Ancestral strain (AS)	Field collection, Fuzhou, China (26°05′N, 119°18′E)		Collected July 2012; maintained at 26°C
Strain, strain background (*Plutella xylostella*)	Hot strain (HS)	This paper		Evolved at 32°C/27°C (12h/12h); ~75 generations
**Strain, strain background (*Plutella*	Cold strain (CS)	This paper		Evolved at 15°C/10°C (12h/12h); ~15 generations

Key resources table.

Reagent type (species) or resource	Designation	Source or reference	Identifiers	Additional information
***xylostella*)**				
Genetic reagent (*Plutella xylostella*)	SODC-MU1	This paper		PxSODC knockout; +1 bp insertion; homozygous at G5
Genetic reagent (*Plutella xylostella*)	SODC-MU2	This paper		PxSODC knockout; +2 bp insertion; homozygous at G5
Genetic reagent (*Plutella xylostella*)	SODC-MU3	This paper		PxSODC knockout; −1 bp deletion; homozygous at G5
Strain, strain background (*E. coli*)	DH5α competent cells	YEASEN, Shanghai, China		Cloning host
Gene (*Plutella xylostella*)	*PxSODC*	*P. xylostella* genome	*Px04C00666*	Cu/Zn SOD; ORF 633 bp, 210 aa
Gene (*Plutella xylostella*)	*PxDnmt1*	*P. xylostella* genome		DNA methyltransferase 1
Recombinant DNA reagent	pESI-Blunt vector	YEASEN, Shanghai, China		Cloning vector
Recombinant protein	Cas9 protein	GenCrispr, Nanjing, China		200 ng/μL in injection mixture
Sequence-based reagent	PxSODC sgRNA	This paper		See Supplementary file 7
Sequence-based reagent	dsDnmt1	This paper		dsRNA for PxDnmt1 RNAi; see Supplementary file 7
Sequence-based reagent	dsEGFP	This paper		Control dsRNA; see Supplementary file 7
Sequence-based reagent	All primers	This paper		Full list in Supplementary file 7
Commercial assay or kit	Eastep® Super Total RNA Extraction Kit	Promega, Shanghai, China		RNA extraction
Commercial assay or kit	Reverse-Transcription System Kit	Promega, Shanghai, China		cDNA synthesis
Commercial assay or kit	2× Taq Pro Universal qPCR Master Mix	Vazyme, Nanjing, China		qRT-PCR
Commercial assay or kit	Phanta® Max Super-Fidelity DNA Polymerase	Vazyme, China		High-fidelity PCR
Commercial assay or kit	Hieff Clone™ Zero TOPO-Blunt Simple	YEASEN, Shanghai, China		TA cloning

Key resources table. (continued)

Key resources table. (continued)

Reagent type (species) or resource	Designation	Source or reference	Identifiers	Additional information
Commercial assay or kit	Cloning Kit TiANamp Genomic DNA Kit	TIANGEN, China		gDNA extraction
Commercial assay or kit	HiScribe™ T7 Quick High Yield RNA Synthesis Kit	New England Biolabs, USA		sgRNA in vitro transcription
Commercial assay or kit	T7 High Yield RNA Transcription Kit	Vazyme, Nanjing, China		dsRNA synthesis for RNAi
Commercial assay or kit	Gel Extraction Kit	Omega Bio-tek, USA		PCR product purification
Commercial assay or kit	SOD activity assay kit	Comin Biotechnology, China		SOD enzyme activity
Commercial assay or kit	O□□ assay kit	Comin Biotechnology, China		Superoxide anion levels
Commercial assay or kit	5-mC ELISA kit	Shanghai Enzyme-linked Biotechnology, China		DNA methylation detection
Chemical compound, drug	Ethylene glycol	Sigma-Aldrich		Supercooling/freezing point assay
Software, algorithm	TWOSEX-MSChart	Chi et al., 2020		Life table analysis; bootstrap 100,000
Software, algorithm	HISAT2 V2.1.0	Kim et al., 2019	RRID:SCR_015530	RNA-seq alignment
Software, algorithm	DESeq2	Bioconductor	RRID:SCR_015687	Differential expression analysis
Software, algorithm	WGCNA v2.0	Langfelder and Horvath, 2008	RRID:SCR_003302	Co-expression network analysis
Software, algorithm	GROMACS 2022.3		RRID:SCR_014565	MD simulations; Amber99sb-ildn
Software, algorithm	AlphaFold2	DeepMind	RRID:SCR_025089	Protein structure prediction
Software, algorithm	IQ-TREE		RRID:SCR_017254	ML phylogenetics; bootstrap 1,000
Software, algorithm	SPSS v23.0	IBM	RRID:SCR_002865	Statistical analysis
Other	Illumina HiSeq4000	Illumina, San Diego, USA		RNA-seq platform
Other	QuantStudio Real-Time PCR System	Thermo Fisher, USA		qRT-PCR
Other	Olympus SZX16 microinjection system	Olympus, Japan		CRISPR egg injection
Other	Nanoliter 2000 microinjector	World Precision Instruments, USA		dsRNA injection

photoperiod, diet) remained identical across treatments. The populations were maintained with non-overlapping generations and a census population size of approximately 500 individuals per replicate.

Prior to the start of the selection experiment, the ancestral population was maintained in the laboratory at 26°C for approximately ~170 generations. The thermal selection experiment was then conducted for approximately three years, encompassing ~75 and ~15 generations for the hot and cold strains, respectively. To minimize maternal effects and ensure that observed differences were due to genetic adaptation rather than developmental plasticity, all populations were reared for two additional generations under common garden conditions (26°C) prior to phenotypic and molecular assays. All six replicate populations per treatment were used for downstream experiments, resulting in 18 experimental cohorts in total.

Development of age-stage-specific two-sex life tables

To study the life history and population fitness of the three different *P. xylostella* strains, age-stage-specific life tables were developed. A total of 90 randomly selected newly laid eggs from each strain were transferred to three 90 mm diameter Petri dishes (30 eggs per dish) and maintained at the favorable temperature (26°C) (Chi et al., 2020). The stage-specific number of individuals was recorded daily (food replaced every two days). During the pupal stage, each pupa was placed in a perforated 1.5 mL centrifuge tube. After eclosion, adults were transferred to 50 mL plastic cups for mating and oviposition and fed with a 10% honey solution. We continuously monitored and recorded daily oviposition and the number of surviving adults within the population until all individuals died.

For the individual life tables, 120 randomly selected newly laid eggs from each strain (i.e., 120 eggs/strain/temperature) were placed under different temperature conditions (favorable, hot, and cold environments). The eggs were individually transferred to 30 mm diameter petri dishes (artificial diet replaced every two days). The number of surviving larvae and pupae was recorded daily, and each pupa was placed individually in a perforated 1.5 ml centrifuge tube. One newly emerged adult female and one newly emerged adult male were placed in a 25 mL plastic cup and fed with a 10% honey solution for mating and oviposition. The number of eggs laid by each adult female was recorded daily until death. The longevity of both males and females was recorded.

Life history and population fitness parameters, including egg duration, larval duration, pupal duration, preadult duration, female and male longevity, oviposition days, fecundity, intrinsic rate of increase (r), finite rate of increase (λ), net reproductive rate (R_0), and mean generation time (T), were calculated based on the recorded data of age-stage-specific two-sex life tables of different strains. The numerical computation was done using the TWOSEX-MSChart software (*https://www.faas.cn/cms/sitemanage/index.shtml?siteId=810640925913080000*) and the bootstrap method with 100,000 replications to obtain standard errors of the fitness parameters. The paired bootstrap (BT) method with 100,000 replications was used to assess pairwise differences among all strains, including comparisons among HS, AS, and CS, as well as among the ancestral and SODC-MU mutant strains under each thermal regime. A P value of less than 0.05 indicates a statistically significant difference (Chi, 1988).

Metabolomic and transcriptomic profiling

All samples for omics profiling were collected after two generations of rearing under common conditions (26°C in climate-controlled chambers) to capture constitutive, genetically based differences between the strains, avoiding confounding effects of immediate physiological plasticity that would occur under thermal stress. The 3rd-instar larval stage was selected as the most actively feeding and rapidly growing stage, where metabolic demands and energetic trade-offs critical for adaptation are most pronounced. Samples collected for metabolomic profiling included: (1) the 3rd-instar larvae from different strains (AS, HS and CS) maintained at the favorable temperature (26°C); and (2) the 2-day-old eggs, 1-day-old 3rd-instar larvae, 2-day-old pupae and newly emerged adults from the ancestral and SODC-MU (MU1 and MU2) strains (see section Deletion of the targeted gene using the CRISPR/Cas9 genome editing) at the favorable temperature. Each biological

replicate consisted of pooled individuals at the same developmental stage. Six independent biological replicates per strain were used for metabolomic profiling and three for transcriptomic profiling. The same sample collection strategy was applied to both analyses, but replicates were collected independently.

Metabolomic profiling

To identify metabolic changes associated with thermal adaptation, we performed targeted metabolomic profiling using UPLC-MS/MS. Stored samples were thawed on ice and weighed (50 ± 2 mg) into 1.5 mL centrifuge tubes, to which three pre-cooled steel balls (3 mm) and 500 μL of pre-cooled 70% methanol (Merck, Germany) were added. Each of the samples was homogenized in a pre-cooled tissue homogenizer (25 HZ, 5 min) (Tissuelyser, Qiagen), and then the homogenized sample was left on ice for 15 min, then centrifuged at 12,000 rpm at 4°C for 10 min. The supernatant was transferred to a new 1.5 mL centrifuge tube and stored overnight at -20°C. The following day, the samples were centrifuged at 12,000 rpm for 3 minutes at 4°C. The supernatant was then collected with a sterile syringe and filtered through a 0.22 μm filter (Waters, USA) into an HPLC sample vial. The instrumental system for data acquisitions mainly used ultra-high performance liquid chromatography and tandem mass spectrometry (multiple reaction monitoring mode). The chromatography and tandem mass spectrometry conditions were as described by Li et al (2021). For all metabolomic comparisons (HS *vs*. AS, CS *vs*. AS, and SODC-MU *vs*. AS), differential metabolites were identified through pairwise comparisons using Student's t-test with false discovery rate (FDR) correction. A multi-criteria threshold of $|\log_2\text{Fold Change}| \geq 1$, VIP (variable importance in projection) ≥ 1, and FDR < 0.05 was applied. All differential metabolites were assigned to different pathways by KEGG analysis.

RNA extraction and cDNA synthesis

To obtain templates for gene cloning and qRT-PCR analysis, total RNA was extracted using the Eastep® Super Total RNA Extraction Kit (Promega, Shanghai) according to the manufacturer's instructions. RNA integrity and quality were assessed using a NanoDrop 2000 spectrophotometer (GE Healthcare, USA) and 2% agarose gel electrophoresis. Total RNA (2000 ng) was reverse transcribed into cDNA using the Reverse-Transcription System Kit (Promega, Shanghai).

Transcriptomic profiling

To identify gene expression changes associated with thermal adaptation, mRNA libraries were constructed for each of the samples and sequenced on the Illumina HiSeq4000 platform (Illumina, San Diego). Raw reads obtained from sequencing were filtered, low quality reads were removed using adapters, and clean reads were obtained for subsequent information analysis. Clean reads were aligned to the *P. xylostella* genome using HISAT2 (V2.1.0) (*http://121.37.197.72:5010*), with sequence alignment performed using the software's default parameters. Gene expression levels were measured using FPKM (fragments per kilobase of transcript per million fragments mapped). The *P*-value was corrected for multiple hypothesis testing following Benjamini and Hochberg (1995). Differential expression analysis between samples was performed using DESeq2. Differentially expressed genes were identified using the criteria of $|\log_2\text{Fold Change}| \geq 1$ and FDR (false discovery rate) < 0.05. All differentially expressed genes were classified into different pathways by KEGG analysis.

Weighted gene co-expression network analysis (WGCNA)

To identify gene modules correlated with differential metabolites between thermally adapted and ancestral strains, we performed weighted gene co-expression network analysis (WGCNA). Genes with an FPKM value below 0.1 were filtered out. The WGCNA package in R (v2.0) was used to calculate weight values and a soft threshold was determined based on the scale-free network principle. A gene clustering tree was constructed based on gene expression correlations, and gene modules were identified based on these clustering relationships. The minimum number of genes per module was set to 30, and the cut height threshold was set to 0.25 to merge potentially similar

modules, with other parameters set to default values. Differential metabolites shared between the hot and cold strains relative to the ancestral strain were used as trait data for correlation analysis, as metabolites represent intermediate molecular phenotypes that bridge gene expression and organismal-level traits, enabling more direct identification of functionally relevant gene modules. Pearson correlations were calculated between each module eigengene and each of the 30 common differential metabolites (29 modules × 30 metabolites = 870 tests). Following standard WGCNA practice, a stringent dual threshold of |correlation coefficient| > 0.8 and $P < 0.05$ was applied to identify significant module-metabolite associations, effectively controlling for false positives (Langfelder and Horvath, 2008). Genes within specific modules were compared with differentially expressed genes and those common to both were considered as candidate genes.

Gene cloning

To identify non-synonymous mutations in candidate genes across the different strains, the following gene sequences were amplified: (1) differentially expressed genes identified from specific modules; and (2) genes from the *PxSODC* gene family. Reference sequences for these genes were obtained from the *P. xylostella* genome database and full-length primers were designed using Primer Premier 6.0 (Supplementary File 7). PCR amplifications were performed using cDNA from the ancestral, hot and cold strains of *P. xylostella* (at least six samples) as templates, using Phanta® Max Super-Fidelity DNA Polymerase (Vazyme, China). The 50 μL PCR reaction mixture contained 2× reaction buffer (25.0 μL), dNTP mix (1.0 μL), 20 μM upstream primer F (2.0 μL), 20 μM downstream primer R (2.0 μL), DNA polymerase (1.0 μL), nuclease-free water (15.0 μL) and cDNA (4.0 μL). Amplification conditions were as follows 95°C for 3 minutes, followed by 35 cycles of 95°C for 15 seconds, 58°C for 15 seconds and 72°C for a gene-specific extension time, with a final extension at 72°C for 5 minutes. The integrity of the PCR products was verified by 2% agarose gel electrophoresis and purified using the Omega gel extraction kit (USA). The purified fragments were cloned into the pESI-Blunt vector using the Hieff CloneTM Zero TOPO-Blunt Simple Cloning Kit (YEASEN, Shanghai, China) and transformed into competent DH5α cells (YEASEN, Shanghai). The ligated product was transferred to DH5α competent cells and plated on LB+100 μg/ml ampicillin plates and incubated overnight at 37°C. A single colony was picked and placed in 500 μL of liquid LB with 100 μg/mL ampicillin. A positive clone was sent to Sangon Biotech (Shanghai, China) for sequencing. Sequence alignments of candidate genes from different strains were performed using Snap Gene software.

Sequence analysis and phylogenetic tree construction

To determine the exons and introns of the target genes, their sequences were aligned with gDNA from the *P. xylostella* genome database. Protein sequences were analyzed using a protein sequence analysis and classification tool (InterPro, *http://www.ebi.ac.uk/interpro/*). The relative molecular masses and isoelectric points of the proteins were predicted using Expasy (*http://expasy.org/tools/dna.html*). The secondary structures of the proteins were predicted using PSIPRED (*http://bioinf.cs.ucl.ac.uk/psipred*). A phylogenetic tree was inferred using the model-based Maximum Likelihood method implemented in IQ-TREE, and the robustness of the tree was verified by bootstrap analysis (bootstrap = 1000 replicates). In the absence of a valid outgroup sequence, the resulting gene tree was presented as unrooted

Molecular dynamics (MD) simulations

To investigate the structural consequences of the identified non-synonymous mutations in *PxSODC* under thermal stress, molecular dynamics (MD) simulations were performed using GROMACS 2022.3. The 3D structures of the wild-type (WT) and mutant (MU) PxSODC proteins were predicted using AlphaFold2. The Amber99sb-ildn force field was applied to the protein systems. Each system was solvated in a cubic box with TIP3P water molecules and neutralized by adding appropriate NaC ions. Energy minimization was performed using the steepest descent algorithm. Subsequently, 100 ps of NVT (constant volume and temperature) equilibration followed by 100 ps of NPT (constant pressure and temperature) equilibration were conducted with a coupling constant of 0.1

ps. Production MD simulations were then run for 100 ns (5,000,000 steps with a 2 fs timestep) at three temperatures: 15°C (288.15 K, cold stress), 26°C (299.15 K, favorable baseline), and 32°C (305.15 K, heat stress). Structural stability and dynamic properties were evaluated using built-in GROMACS analysis tools, including root mean square deviation (RMSD), solvent accessible surface area (SASA), and intramolecular hydrogen bond number. The 26°C simulation served as the physiological baseline for interpreting stress-induced structural changes.

qRT-PCR analysis

To validate transcriptomic data and quantify expression levels of candidate genes across strains and temperature conditions, we collected samples as follows: (1) we randomly selected 22 genes from the transcriptomes of the 3rd-instar larvae of ancestral, hot, and cold strains to validate the transcriptome data; (2) we collected samples from the eggs, 3rd-instar larvae, pupae and adult males and females of the ancestral, hot, cold and SODC-MU (MU1 and MU2) strains to assess the transcription levels of genes including *PxSODC*, *Px04C00505*, *Px13C00423*, *Px20C00248*, *Px15C00224* and *Px15C00223*; (3) we collected the 3rd-instar larvae of the ancestral and hot strains exposed to different high temperature treatments (32°C, 34°C, 36°C) to analyze the transcription levels of the above-mentioned genes; and (4) we collected the 3rd-instar larvae of the ancestral and cold strains exposed to different low temperature treatments (12°C, 10°C, 8°C) for similar assessments.

qRT-PCR primers were designed using Primer Premier 6.0, with *PxRPL*[32] as the reference gene (Supplementary File 7). The reaction mixture of 20 μL contained 10 μL 2× Taq Pro Universal qPCR Master Mix (Vazyme, Nanjing, China), 0.4 μL of each primer, 7.15 μL nuclease-free water and 2.0 μL cDNA. The QuantStudio Real-Time PCR System (Thermo, USA) protocol was as follows: 95°C for 30 s; 40 cycles of 95°C for 10 s, 60°C for 30 s; followed by melting curve analysis of 95°C for 15 s, 60°C for 1 min, 95°C for 15 s. Each sample contained 3 biological replicates and 3 technical replicates, and the relative expression of genes was calculated using the $2^{-\Delta\Delta Ct}$ method.

Deletion of the targeted gene using the CRISPR/Cas9 genome editing

To functionally validate the role of *PxSODC* in thermal adaptation, we generated stable homozygous mutant strains of *P. xylostella* with the *PxSODC* gene deleted using the CRISPR/Cas9 system. The target site was designed based on the 5'-N20NGG-3' motif (underscore indicates PAM sequence), and the potential off-target effect of sgRNAs was predicted using Cas-OFFinder (*http://www.rgenome.net/cas-offinder*). The in vitro transcription template for sgRNA was generated from a single nucleotide strand under the following conditions: 95°C for 3 min, followed by 35 cycles of 95°C for 15 s, 68°C for 15 s and 72°C for 30 s, with a final extension at 72°C for 5 min. The amplified product was purified by gel extraction. The sgRNA was obtained by in vitro transcription of the gel-purified product using the HiScribe™ T7 Quick High Yield RNA Synthesis Kit (New England Biolabs, USA). The reaction mixture contained 2.5 μL NTP buffer mix, 0.5 μL T7 RNA polymerase mix, 65 ng gel-purified product, made up to 5 μL with nuclease-free water. After overnight incubation at 37°C, 0.5 μL of DNase was added to remove DNA and the product was incubated at 37°C for 20 minutes to yield sgRNA. The sgRNA was purified by phenol-chloroform extraction and stored at -80°C.

We prepared a 10 μL reaction mixture containing 300 ng/μL sgRNA and 200 ng/μL Cas9 protein (GenCrispr, Nanjing), 1 μL 10× reaction buffer and nuclease-free water to make up to 10 μL and incubate at 37°C for 25 minutes. The mixture was injected into freshly laid eggs using the Olympus SZX16 microinjection system (Olympus, Japan) and the entire microinjection was completed within 30 minutes of eggs being laid. After injection, the eggs were placed in a Petri dish and the number of eggs hatched was recorded. Adult gDNA was extracted using the TiANamp Genomic DNA Kit (TIANGEN, China). Specific primers were designed for PCR amplification (Supplementary File 7), with conditions as follows: 95°C for 3 min, followed by 34 cycles of 95°C for 15 s, 58°C for 15 s and 72°C for 15 s, with a final extension at 72°C for 5 min. The sequence of the PCR products was checked by Sangon Biotech (Shanghai) Co., Ltd.

The injected eggs were referred to as the G0 generation. These were reared to adulthood, crossed with the ancestral (non-injected) adults and used to extract genomic DNA from G0 adults after oviposition (the resulting progeny representing the G1 generation). PCR products flanking the two sgRNA target sites were amplified as mentioned above to determine genotypes and identify heterozygotes (individuals with double peaks in the sequence chromatogram starting from the sgRNA target site). The G1 generation was self-crossed to produce the G2 generation, and all G1 adults were genotyped based on PCR amplification for individual identification. G2 progeny derived from G1 heterozygotes with the same allelic mutation were selected. The G2 generation was then self-crossed to produce the G3 generation, retaining those with the same type of homozygous mutations to establish homozygous lines. If the G3 generation remained heterozygous, self-crossing continued until homozygous mutations were obtained (Wang et al., 2020). By the end, three mutants were obtained and called SODC-MU (MU1, MU2 and MU3) strains.

RNA interference mediated silencing of target genes

To assess the role of *PxDnmt1* in thermal tolerance, we silenced its expression using RNA interference. Gene-specific primers containing T7 promoter sequences were designed (Supplementary File 7), and PCR was performed using total *P. xylostella* cDNA as a template. The PCR products were purified using a gel extraction kit. Double-stranded RNA (dsRNA) was synthesized by in vitro transcription using the T7 High Yield RNA Transcription Kit (Vazyme, Nanjing, China). The dsRNA was diluted to 2 μg/μL using DEPC-treated water (Beyotime, Shanghai, China). A volume of 500 nL diluted dsRNA (ds*EGFP* or ds*Dnmt1*) was injected into pupae using a Nanoliter 2000 microinjector (World Precision Instruments LLC, USA). Total RNA was extracted 24 hours after injection and reverse transcribed to cDNA. Gene knockdown efficiency was analyzed by qPCR using pupae injected with ds*EGFP* as controls. The experiment was performed in three independent biological replicates (Zhou et al., 2024).

Assessing the response to high temperature

To assess the response of different *P. xylostella* strains (ancestral strain, hot strain and mutants) to extremely high temperatures, 2-day-old eggs, 1-day-old 3rd-instar larvae and 2-day-old pupae were individually placed in 90 mm diameter Petri dishes. Adult females and males were placed individually in perforated 1.5 mL centrifuge tubes. Based on a preliminary trial on the stage-specific temperature tolerance limit of *P. xylostella* (eggs, larvae, pupae, and both male and female adults of the ancestral and hot strains were placed in different temperature environments ranging from 40 to 45°C), pupae from the ancestral and mutant strains were exposed to 43°C while eggs, larvae, and adults were exposed to 42°C for periods ranging from 30 to 180 minutes. After treatment, all replicate samples were transferred to an environment maintained at 26°C, where survival was observed and recorded. Survival was defined as the successful development of eggs, larvae and pupae to the next stage, while adults had to show movement of an appendage or mouthparts. Experiments were performed with six biological replicates, with each replicate contained 20 individuals.

We randomly selected 20 female adults injected with dsRNA to determine their critical thermal maximum (CTMax). A thermistor probe (Omega, USA) was inserted into a 1.5 mL centrifuge tube, which was suspended inside a 50 mL centrifuge tube with the opening sealed with cotton. This assembly was then placed in a 2 L glass beaker containing 1000 mL water, with the beaker top sealed with insulating foam board. The entire setup was positioned on a thermostatically controlled magnetic stirrer, where the temperature inside the 1.5 mL tube was increased at a constant rate of 0.5°C/min. When the temperature reached 26°C, female adults were quickly transferred into the 1.5 mL centrifuge tube containing the temperature probe, and their behavioral responses were continuously monitored as temperature increased. The CTMax was recorded when moths exhibited spasms, lost their crawling or flying ability, and remained motionless at the bottom of the tube, typically lying ventral side up (in most cases) or dorsal side up (in fewer instances). Although antennae and limbs might still exhibit slight tremors at this point, the insects typically died within seconds (Li et al., 2024b).

Measurement of the supercooling and freezing points

To investigate the cold hardiness of different *P. xylostella* strains (including the ancestral, cold and mutant trains), we randomly selected 40 pupae from each strain to examine their supercooling and freezing points. A thermistor probe from a subcooling point tester (Omega, USA) was attached to a pupa, secured with conductive tape and placed in a centrifuge tube, with the tube mouth sealed by cotton. The centrifuge tubes were then placed in a 50 mL plastic cup filled with ethylene glycol (antifreeze), and the cup was stored in an ultra-low temperature freezer set at -70°C, with the temperature first dropping rapidly and then decreasing at a rate of 0.10°C per second until the supercooling point was reached. By recording temperature changes at intervals of every second, the supercooling and freezing points of pupae were determined based on the inflection point of body temperature. The same experimental approach was also applied to *P. xylostella* injected with dsRNA.

Detection of oxidative stress indicator

To assess the impact of thermal adaptation and *PxSODC* deletion on oxidative stress, we measured superoxide dismutase (SOD) activity and superoxide anion (O^-) levels. Samples were collected in the following conditions: (1) the eggs, 3rd-instar larvae, pupae, and adult males and females of the ancestral, hot, cold, and SODC-MU (MU1 and MU2) strains at the favorable temperature (26°C); (2) the 3rd-instar larvae of the ancestral, hot, and SODC-MU (MU1 and MU2) strains after 2 hours of heat stress at 32°C, 34°C, and 36°C; and (3) the 3rd-instar larvae of the ancestral, cold, and SODC-MU (MU1 and MU2) strains after 2 hours of cold stress at 12°C, 10°C, and 8°C. The experiment was performed with four independent biological replicates. The levels of SOD and O_2^- were measured using commercial assay kits (Comin, China) according to the manufacturer's instructions.

Detection of 5-methylcytosine concentration

To evaluate the effect of *PxDnmt1* silencing on DNA methylation levels, pupae and female adults were collected for detection of 5-methylcytosine (5-mC) concentration after injection with dsRNA. The levels of 5-mC were measured using a commercial insect 5-methylcytosine (5-mC) ELISA detection kit (Shanghai Enzyme-linked Biotechnology Co., Ltd., China) according to the manufacturer's instructions. The experiment was performed with four independent biological replicates.

Data analysis

Statistical analyses for life table parameters, metabolomic data, and transcriptomic data are described in their respective sections above. For all other experimental data (qRT-PCR, SOD activity, O_2^- levels, DNA methyltransferase activity, 5-mC concentration, stage-specific survival rates, and supercooling/freezing points), analyses were performed using SPSS version 23.0. The Shapiro-Wilk test was used to assess normality of data distribution. For normally distributed data, two-group comparisons were analyzed using independent samples t-tests, while comparisons

involving three or more groups were analyzed using one-way ANOVA followed by Tukey's test (homogeneous variances) or Tamhane's T2 test (unequal variances). For non-normally distributed data, the Mann-Whitney test (two groups) or Kruskal-Wallis test (three or more groups) was used. A *P* value of less than 0.05 was considered statistically significant in all cases (Lei et al., 2024).

Figure supplements

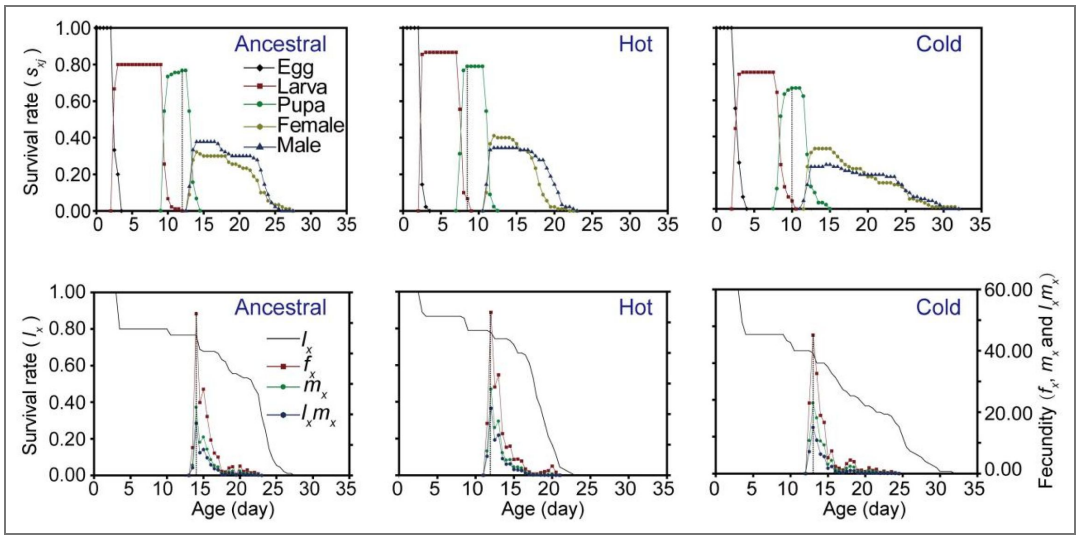

Figure 1-figure supplement 1. Phenotypic fitness variation in the ancestral, hot and cold strains of *P. xylostella*. The curves show the age-stage survival rate (s_{xj}), age-specific survival rate (l_x), female age-specific fecundity (f_{xj}), and population age-specific fecundity (m_x) of the ancestral, hot, and cold strains.

Figure 2-figure supplement 1. Metabolomic analysis of the 3rd-instar larvae across the ancestral, hot and cold strains of *P. xylostella*.

(A) Inter-sample correlation heat map of the metabolites. Z-score standardized values for each of the metabolites were used in clustering analysis. The color bar indicates an increase in the content of each metabolite, scaling from blue to red. (B) KEGG functional classification of differential metabolites between the hot/cold and ancestral strains. (C) Correlation analysis of differential metabolites between the hot/cold and ancestral strains. Pearson's correlation coefficient (*r*) was used to evaluate the biological correlation between different replicates.

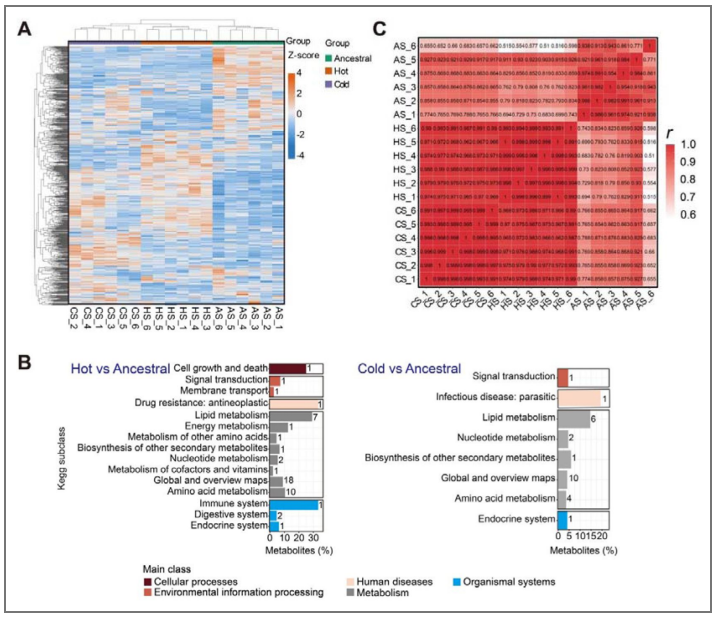

Figure 3-figure supplement 1. Transcriptomic analysis of the 3rd-instar larvae across the ancestral, hot and cold strains of *P. xylostella*.

(A) qRT-PCR validation of transcriptome data. (B) Soft threshold selection in WGCNA. Left: The soft threshold selection graph. Right: The mean connectivity of genes under different soft thresholds. (C) Correlation heat map showing the association of the 29 modules with common differential metabolites between the hot/cold and ancestral strains.

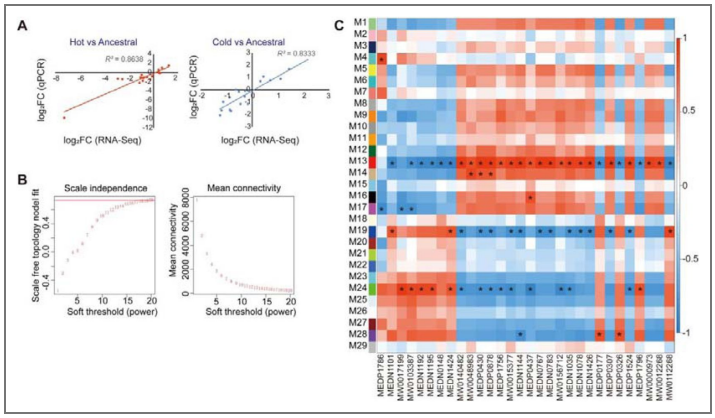

Figure 5-figure supplement 1. **Bioinformatic prediction and analysis of the *PxSODC* gene sequence.**

(A) The structure of the *PxSODC* gene, consisting of three exons and two introns. (B) Secondary structure prediction of PxSODC. Yellow represents strand, pink represents helix, and grey represents coil. (C) Unrooted Maximum Likelihood phylogenetic tree of PxSODC based on amino acid sequences. The tree was inferred using IQ-TREE with 1000 bootstrap replicates, with a blue dot marking the position of *P. xylostella*.

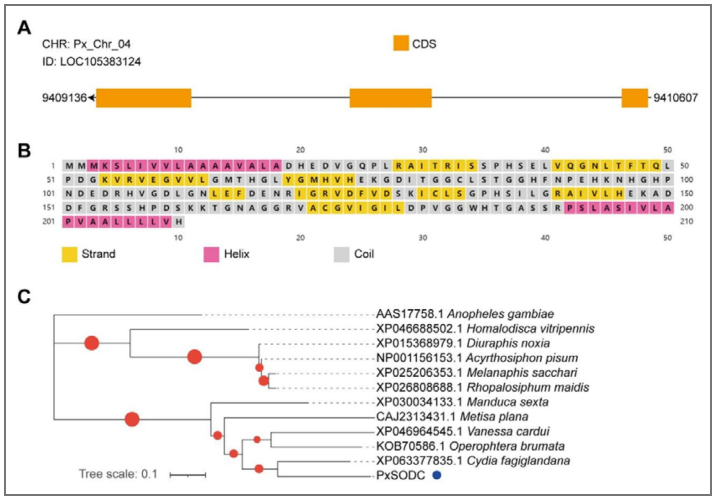

Figure 5-figure supplement 2. **Spatio-temporal expression patterns of the *PxSODC* gene in the ancestral, hot and cold strains of *P. xylostella*.**

(A) Stage-specific profiling of the *PxSODC* expression patterns among different strains in the favorable temperature environment (26°C), and One-way ANOVA with Tukey's test was used for comparison ($p < 0.05$). (B) Expression levels of *PxSODC* in the 3rd-instar larvae of the ancestral and hot strains after 2 h exposure to different high temperature environments (32°, 34°, 36°, 38° and 40°C), and t-test was used for comparison ($p < 0.05$). (C) Expression levels of *PxSODC* in the 3rd-instar larvae of the ancestral and cold strains after 2 h exposure to different low temperature environments (12°, 10°, 8°, 6° and 4°C), and t-test was used for comparison ($p < 0.05$). Data are presented as mean±SEM, with $n = 3$ biologically independent samples for each data point.

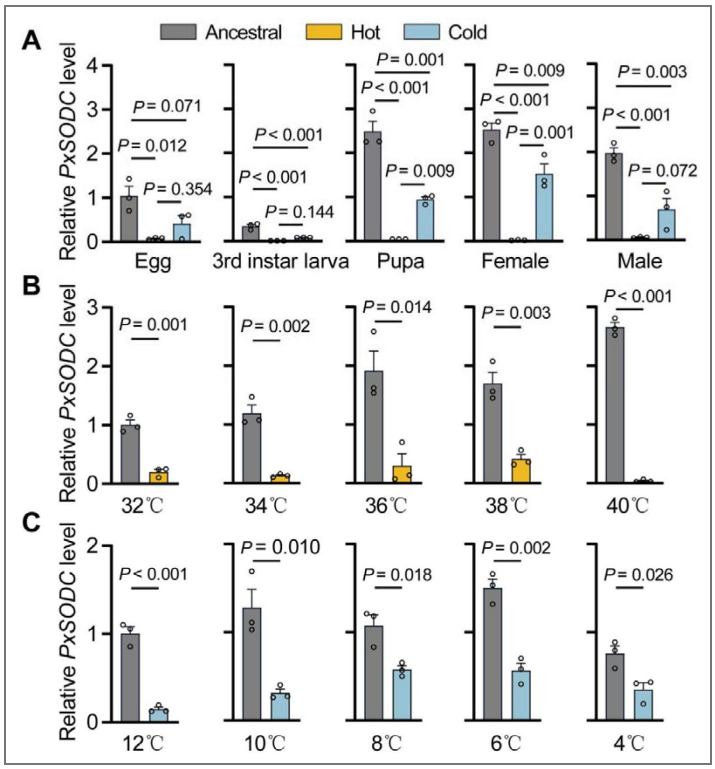

Figure 5-figure supplement 3. Molecular dynamics simulations of wild-type (WT) and mutant (MU) PxSODC proteins at 15°C, 26°C, and 32°C.

The favorable temperature (26°C) served as the physiological baseline. (A-C) RMSD time-series trajectories over 100 ns at 15°C (A), 26°C (B), and 32°C (C). (D) Solvent accessible surface area (SASA) across three temperatures, demonstrating the more compact structure of MU at 15°C and 26°C. (E) Number of intramolecular hydrogen bonds across three temperatures. Under cold stress (15°C), MU actively increased hydrogen bonds compared to the 26°C baseline, whereas WT lost bonds. Under heat stress (32°C), MU fully maintained its bond count. Data in (D) and (E) are presented as mean ± SE from 100 ns simulations.

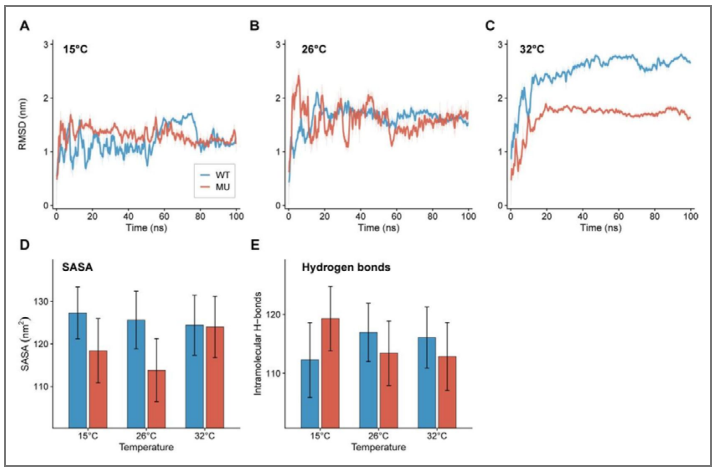

Figure 5-figure supplement 4. CRISPR/Cas9-mediated mutagenesis of the *PxSODC* gene.

Black underlines indicate the sgRNA target sequence in the second exon, yellow underlines highlight the PAM recognition site, dashes indicate deleted base sequences and blue letters indicate inserted base sequences.

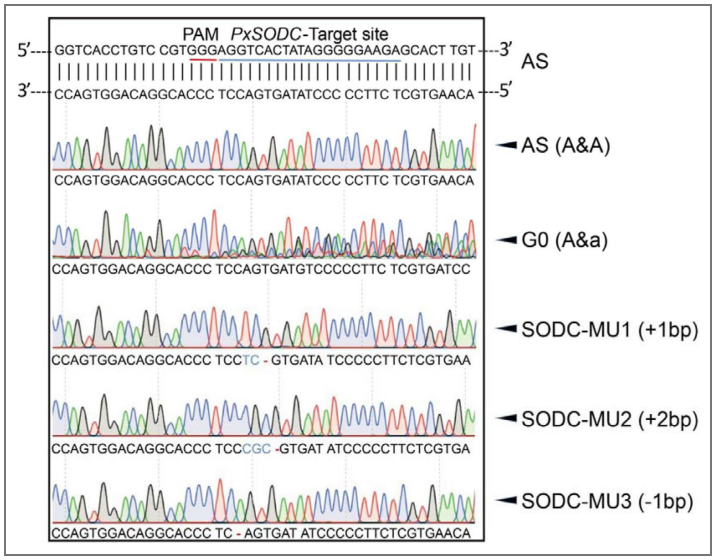

Figure 5-figure supplement 5. Comparison of the survival rates (s_{xj} and l_x) and female fecundity (f_x and m_x) of *P. xylostella* strains, showing the role of *PxSODC* in the temperature adaptation.

(A) Age-stage survival rates (s_{xj}) of the ancestral and mutant strains (AS, SODC-MU1, SODC-MU2 and SODC-MU3) in different temperature environments. (B) Age-specific survival rates (l_x), female age-specific fecundity (f_x), and population age-specific fecundity (m_x) of the ancestral and mutant strains (AS, SODC-MU1, SODC-MU2 and SODC-MU3) in different temperature environments.

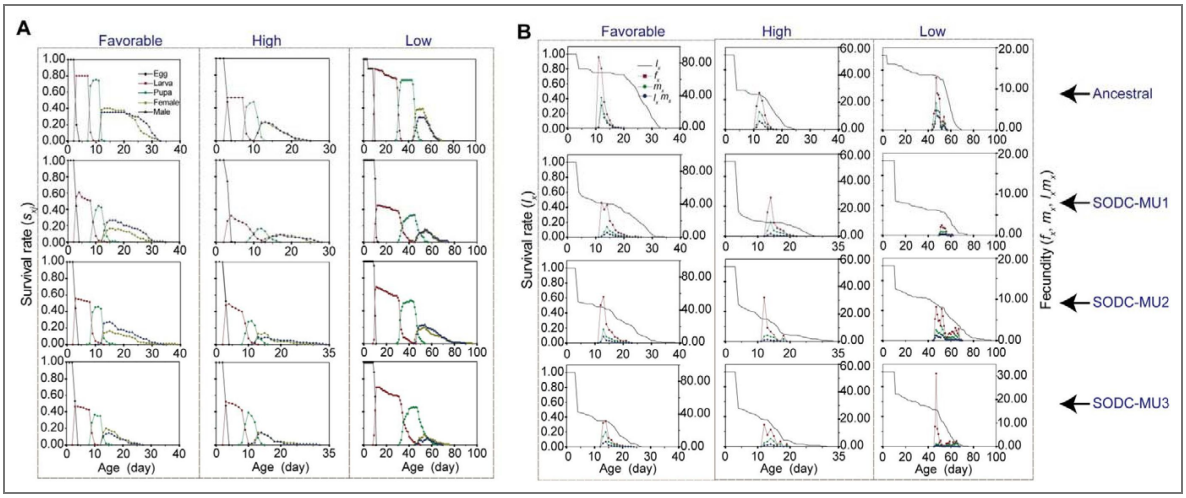

Figure 7-figure supplement 1. Metabolomic analysis of different developmental stages in the ancestral and mutant strains of *P. xylostella*.

(A) Classification of metabolites. A total of 608 metabolites were detected in the ancestral and mutant strains (AS and SODC-MU1/SODC-MU2). (B) Principal component analysis (PCA) of the 608 metabolites in the ancestral and mutant strains (AS and SODC-MU1/SODC-MU2). PC1 and PC2 represent the first and second principal components, respectively. (C) Volcano plot showing down-regulated (blue dots) and up-regulated (red dots) metabolites identified in the mutant strains compared to the ancestral strain). (D) Venn diagram showing common and unique differential metabolites between the ancestral and mutant strains at different developmental stages.

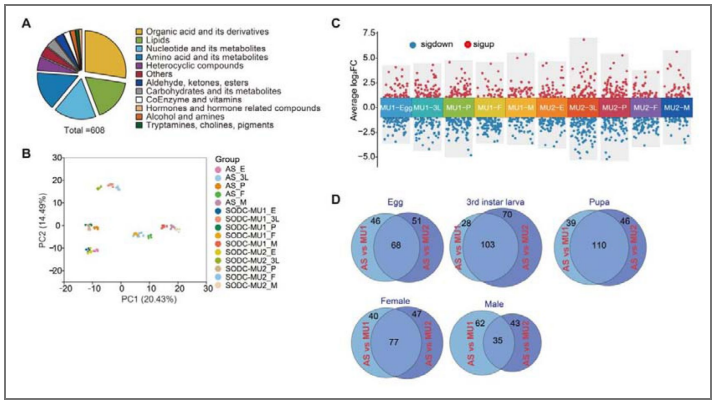

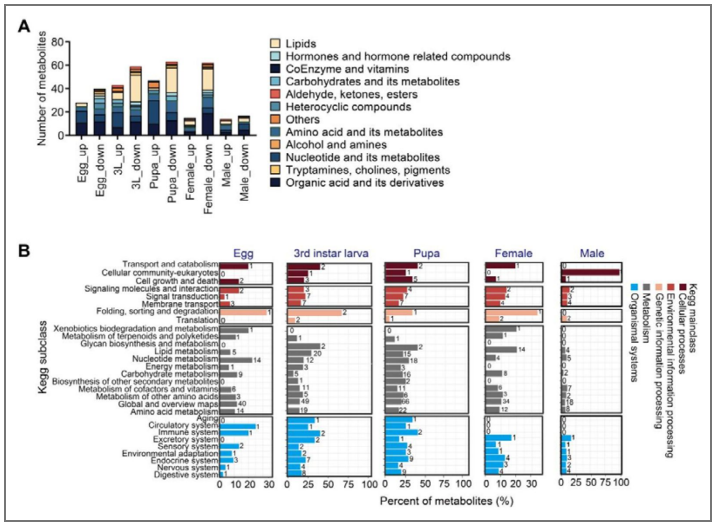

Figure 7-figure supplement 2. Differential metabolite classification and functional analysis in the ancestral and mutant strains across different developmental stages of *P. xylostella*.

(A) Classification of differential metabolites between the ancestral and mutant strains at different developmental stages. (B) KEGG function classification of differential metabolites in the mutant strains compared to the ancestral strain. The vertical axis represents the names of the KEGG pathways and the horizontal axis indicates the number of differential metabolites annotated to each pathway and their proportion of the total metabolites annotated to that pathway.

Acknowledgements

This work was financially supported by the central government-guided local science and technology development project (2022L3087), the Fujian Natural Science Fund for Distinguished Young Scholars (2022J06013), and the research project grants of Fujian Agriculture and Forestry University (KFXH23021, KFB24114A), the State Key Laboratory of Agriculture and Forestry Biosecurity, the International Joint Research Laboratory of Ecological Pest Control, Ministerial and Provincial Joint Innovation Centre for Safety Production of Cross-Strait Crops, and the "111" Program in China.

Additional information

Author contributions

Gaoke Lei, Conceptualization, Data curation, Methodology, Investigation, Writing – original draft;

Huiling Zhou, Conceptualization, Data curation, Methodology, Investigation, Writing – original draft;

Zongyao Ma, Data curation, Formal analysis, Investigation, Methodology;

Yating Duan, Data curation, Formal analysis, Investigation, Methodology;

Yanting Chen, Conceptualization, Methodology;

Fengluan Yao, Conceptualization, Methodology;

Minsheng You, Conceptualization, Data curation, Methodology, Writing – original draft, Writing – review and editing;

Liette Vasseur, Supervision, Writing – review and editing;

Geoff M. Gurr, Supervision, Writing – review and editing;

Shijun You, Conceptualization, Data curation, Methodology, Project administration, Supervision, Writing – original draft, Writing – review and editing.

Funding

Funder	Grant reference number	Author
Central Government-guided Local Science and Technology Development Project	2022L3087	Shijun You
Fujian Natural Science Fund for Distinguished Young Scholars	2022J06013	Shijun You
Fujian Agriculture and Forestry University	Research project grant KFXH23021	Shijun You
Fujian Agriculture and Forestry University	Research project grant KFB24114A	Shijun You

Author ORCID iDs

Liette Vasseur: https://orcid.org/0000-0001-7289-2675
Shijun You: https://orcid.org/0000-0001-7340-1524

Additional files

Supplementary File 1. Life table parameters of the ancestral, hot and cold strains of *P. xylostella* at the favorable temperature (26°C).

Supplementary File 2. Candidate genes linked to thermal adaptation in DBM.

Supplementary File 3. Population fitness parameters of the ancestral strain (AS) and SODC-mutant strains of DBM under the constant favorable environment (26°C).

Supplementary File 4. Populaion fitness parameters of the ancestral strain (AS) and mutant strains of DBM under the hot environment (32°C/27°C:12 h/12 h).

Supplementary File 5. Population fitness parameters of the ancestral strain (AS) and mutant strains of DBM under the cold environment (15°C/10°C:12 h/12 h).

Supplementary File 6. Information on the *PxSODC* homologous genes identified in the transcriptome.

Supplementary File 7. The primers used in this study.

Figure 1—Source Data 1. Raw data for stage-specific thermal tolerance and pupal supercooling/freezing points of temperature-adapted strains.

Figure 5—Source Data 1. Raw data for thermal tolerance phenotypes of *PxSODC* knockout strains.

Figure 6—Source Data 1. Raw data for SOD enzyme activity and superoxide anion (OCC) levels across strains, developmental stages, and temperature conditions.

Figure 7—Source Data 1. Raw data for *PxDnmt1* expression, DNA methyltransferase activity, and effects of *PxDnmt1* silencing on thermal tolerance.

Appendix 1: "Detailed age-stage survival and fecundity analysis"

To characterize how thermal adaptation affects population dynamics across different life stages, we generated curves of the age-stage specific survival rate (s_{xj}), age-specific survival rate (l_x), female age-specific fecundity (f_x), and population age-specific fecundity (m_x) from the age-stage, two-sex life tables of the hot strain (HS), cold strain (CS), and ancestral strain (AS) (Figure 1–figure supplement 1). These curves capture stage-specific variation in survival and fecundity that summary life table parameters alone may obscure, providing a more detailed view of how thermal selection shapes life history trajectories at each developmental stage. The maximum daily survival rates at the pre-adult stages of HS and AS were significantly higher than that of CS (HS = 78.9%, AS = 76.7%, CS = 66.7%; Supplemental Table S1). The peak daily fecundity of HS and AS was also higher than that of CS (HS = 53.22, AS = 53.00, CS = 45.10 eggs per female).

Appendix 2: "Life table analysis of *PxSODC* mutant strains"

Age-stage, two-sex life tables were constructed for the ancestral strain and the three SODC-MU mutant (MU1, MU2, MU3) strains under constant favorable (26°C), hot (32°C/27°C) and cold (15°C/10°C) environments to examine their phenotypic traits including development, survival, fecundity and fitness (Figure 5–figure supplement 5; *Supplementary File 3-5*). Overall, the three mutant strains had a prolonged development time (T), lower survival rates (s_{xj} and l_x), and reduction in the fecundity (f_x and m_x) and population fitness parameters (r, λ, R_0) compared to the ancestral strain. The observed change in these parameters indicated that the loss of *PxSODC* gene function significantly affected the life history and population fitness of *P. xylostella*, particularly in the hot/cold environments. Prolonged developmental time and reduced fecundity suggest that the physiological functions of the mutant strains may be damaged when exposed to both high and low temperature conditions.

Appendix 3: "Metabolomic profiling of *PxSODC* mutant strains"

To explore the metabolic networks associated with the *PxSODC* gene in *P. xylostella* and better understand the biological functions underlying their complex relationships, we performed an untargeted metabolomic analysis on the ancestral and mutant (SODC-MU1 and SODC-MU2) strains at different developmental stages. We detected 608 metabolites across the strains, including 167

organic acids and their derivatives, 102 nucleotides and their metabolites, 102 lipids, 92 amino acids and their metabolites, 33 heterocyclic compounds, 24 carbohydrates and their metabolites, and 88 other metabolites (Figure 7–figure supplement 1A). Principal component analysis (PCA) revealed a distinction between the ancestral and mutant strains along the first component (PC1). However, a trend of clustering was observed in the 3rd-instar larvae of ancestral and SODC-MU1 strains and the male adults of ancestral and SODC-MU2 strains, suggesting that the difference at these developmental stages may be driven by a few key metabolites (Figure 7–figure supplement 1B). Compared to ancestral strain, different metabolites were identified in the eggs, 3rd-instar larvae, pupae, female adults and male adults of mutant strains (Figure 7–figure supplement 1C). The mutant strains had 68, 103, 110, 77 and 35 common differential metabolites compared to the ancestral strain at different developmental stages of *P. xylostella* (Figure 7–figure supplement 1D). In addition, the lipid content significantly decreased in the 3rd-instar larvae, pupae and female adults, while the content of nucleotides and their metabolites increased in the eggs, 3rd-instar larvae and pupae following deletion of the *PxSODC* gene in *P. xylostella* (Figure 7–figure supplement 2A). The up-regulation and down-regulation of various metabolites may be associated with the antioxidant function of *PxSODC*. We observed that the deletion of *PxSODC* gene could lead to elevated levels of the $O^{\cdot-}$ within *P. xylostella* (Figure 6I).

We then performed enrichment analysis of differential metabolite KEGG pathways for the SODC-MU (MU1 and MU2) eggs, 3rd-instar larvae, pupae, female adults and male adults resulting in these differential metabolites wre distributed in 23, 28, 28, 22, and 18 pathways, respectively. They were mainly involving lipid metabolism, nucleotide metabolism, carbohydrate metabolism, cofactor and vitamin metabolism, and amino acid metabolism (Figure 7–figure supplement 2B). These pathways were related to the *PxSODC* gene and might have contributed to the temperature-adaptive capacity in *P. xylostella* through the regulation of biological functions/processes in different temperature environments.

References

Bale JS, Masters GJ, Hodkinson ID, Awmack C, Bezemer TM, Brown VK, Butterfield J, Buse A, Coulson JC, Farrar J (2002) Herbivory in global climate change research: direct effects of rising temperature on insect herbivores. *Glob Change Biol* **8**:1-16 https://doi.org/10.1046/j.1365-2486.2002.00451.x

Barros-Cordeiro KB, Bao SN, Pujol-Luz JR (2014) Intra-puparial development of the black soldier-fly, *Hermetia illucens*. *J Insect Sci* **14**:83 https://doi.org/10.1093/jis/14.1.83 | PubMed

Belfield EJ, Ding ZJ, Jamieson FJC, Visscher AM, Zheng SJ, Mithani A, Harberd NP (2018) DNA mismatch repair preferentially protects genes from mutation. *Genome Res* **28**:66-74 https://doi.org/10.1101/gr.219303.116 | PubMed

Benjamini Y, Hochberg Y (1995) Controlling the false discovery rate: A practical and powerful approach to multiple testing. *J R Stat Soc Ser B* **57**:289-300 https://doi.org/10.1111/j.2517-6161.1995.tb02031.x

Bhutani N, Burns David M, Blau Helen M (2011) DNA demethylation dynamics. *Cell* **146**:866-872 https://doi.org/10.1016/j.cell.2011.08.042 | PubMed

Bittner N, Hundacker J, Achotegui-Castells A, Anderbrant O, Hilker M (2019) Defense of Scots pine against sawfly eggs (*Diprion pini*) is primed by exposure to sawfly sex pheromones. *Proc Natl Acad Sci U S A* **116**:24668-24675 https://doi.org/10.1073/pnas.1910991116 | PubMed

Block W (1997) Cold tolerance of insects and other arthropods. *Phil Trans R. Soc Lond B Biol Sci* **326**:613-633 https://doi.org/10.1098/rstb.1990.0035

Bremer J (1983) Carnitine-metabolism and functions. *Physiol Rev* **63**:1420-1480 https://doi.org/10.1152/physrev.1983.63.4.1420 | PubMed

Burc E, Girard-Tercieux C, Metz M, Cazaux E, Baur J, Koppik M, Rêgo A, Hart AF, Berger D (2025) Life-history adaptation under climate warming magnifies the agricultural footprint of a cosmopolitan insect pest. *Nat Commun* **16**:827 https://doi.org/10.1038/s41467-025-56177-2 | PubMed

Chen Y, Liu Z, Régnière J, Vasseur L, Lin J, Huang S, Ke F, Chen S, Li J, Huang J (2021) Large-scale genome-wide study reveals climate adaptive variability in a cosmopolitan pest. *Nat Commun* **12**:1-11 https://doi.org/10.1038/s41467-021-27510-2 | PubMed

Chi H (1988) Life-table analysis incorporating both sexes and variable development rates among individuals. *Env Entomol* **17**:26-34 https://doi.org/10.1093/ee/17.1.26

Chi H, You M, Atlıhan R, Smith CL, Kavousi A, Özgökçe MS, Güncan A, Tuan SJ, Fu JW, Xu YY, *et al.* (2020) Age-Stage, two-sex life table: an introduction to theory, data analysis, and application. *Entomol Gen* **40**:103-124 https://doi.org/10.1127/entomologia/2020/0936

Deutsch CA, Tewksbury JJ, Huey RB, Sheldon KS, Ghalambor CK, Haak DC, Martin PR (2008) Impacts of climate warming on terrestrial ectotherms across latitude. *Proc Natl Acad Sci U S A* **105**:6668-6672 https://doi.org/10.1073/pnas.0709472105 | PubMed

Emre I, Kayis T, Coskun M, Dursun O, Cogun HY (2013) Changes in antioxidative enzyme activity, glycogen, lipid, protein, and malondialdehyde content in cadmium-treated *Galleria mellonella* Larvae. *Ann. Entomol. Soc Am* **106**:371-377 https://doi.org/10.1603/an12137

Furlong MJ, Wright DJ, Dosdall LM (2013) Diamondback moth ecology and management: problems, progress, and prospects. *Annu Rev Entomol* **58**:517-541 https://doi.org/10.1146/annurev-ento-120811-153605 | PubMed

Gibert P, Debat V, Ghalambor CK (2019) Phenotypic plasticity, global change, and the speed of adaptive evolution. *Curr Opin Insect Sci* **35**:34-40 https://doi.org/10.1016/j.cois.2019.06.007 | PubMed

Gibson G, Barghi N, Tobler R, Nolte V, Jakšić AM, Mallard F, Otte KA, Dolezal M, Taus T, Kofler R, *et al.* (2019) Genetic redundancy fuels polygenic adaptation in *Drosophila*. *PLoS Biol* **17**:e3000128 https://doi.org/10.1371/journal.pbio.3000128 | PubMed

Halsch CA, Shapiro AM, Fordyce JA, Nice CC, Thorne JH, Waetjen DP, Forister ML (2021) Insects and recent climate change. *Proc Natl Acad Sci U S A* **118**:e2002543117 https://doi.org/10.1073/pnas.2002543117 | PubMed

Harvey JA, Heinen R, Gols R, Thakur MP (2020) Climate changeCmediated temperature extremes and insects: From outbreaks to breakdowns. *Glob Change Biol* **26**:6685-6701 https://doi.org/10.1111/gcb.15377 | PubMed

Hoffmann AA, Sgro CM (2011) Climate change and evolutionary adaptation. *Nature* **470**:479-485 https://doi.org/10.1038/nature09670 | PubMed

IPCC (2023) Climate Change 2023: Synthesis Report. Geneva, Switzerland: IPCC.

Islam MN, Rauf A, Fahad FI, Emran TB, Mitra S, Olatunde A, Shariati MA, Rebezov M, Rengasamy KRR, Mubarak MS (2022) Superoxide dismutase: an updated review on its health benefits and industrial applications. *Crit Rev Food Sci Nutr* **62**:7282-7300 https://doi.org/10.1080/10408398.2021.1913400 | PubMed

Kaiser A, Hartzendorf S, Wobschall A, Hetz SK (2010) Modulation of cyclic CO(2) release in response to endogenous changes of metabolism during pupal development of *Zophobas rugipes* (Coleoptera: Tenebrionidae). *J Insect Physiol* **56**:502-512 https://doi.org/10.1016/j.jinsphys.2009.06.010 | PubMed

Langfelder P, Horvath S (2008) WGCNA: an R package for weighted correlation network analysis. *BMC Bioinform* **9**:559 https://doi.org/10.1186/1471-2105-9-559 | PubMed

Lawlor JA, Comte L, Grenouillet G, Lenoir J, Baecher JA, Bandara RMWJ, Bertrand R, Chen IC, Diamond SE, Lancaster LT, *et al.* (2024) Mechanisms, detection and impacts of species redistributions under climate change. *Nat Rev Earth Environ* **5**:351-368 https://doi.org/10.1038/s43017-024-00527-z

Lei G, Huang J, Zhou H, Chen Y, Song J, Xie X, Vasseur L, You M, You S (2024) Polygenic adaptation of a cosmopolitan pest to a novel thermal environment. *Insect Mol Biol* **33**:387-404 https://doi.org/10.1111/imb.12908 | PubMed

Lei G, Zhou H, Chen Y, Vasseur L, Gurr GM, You M, You S (2023) A very long-chain fatty acid enzyme gene, PxHacd2 affects the temperature adaptability of a cosmopolitan insect by altering epidermal permeability. *Sci Total Environ* **891**:164372 https://doi.org/10.1016/j.scitotenv.2023.164372 | PubMed

Li J, Holford P, Beattie GAC, Wu S, He J, Tan S, Wang D, He Y, Cen Y, Nian X (2024a) Adipokinetic hormone signaling mediates the enhanced fecundity of *Diaphorina citri* infected by 'Candidatus Liberibacter asiaticus'. *eLife* **13**:RP93450 https://doi.org/10.7554/eLife.93450 | PubMed

Li S, Deng B, Tian S, Guo M, Liu H, Zhao X (2021) Metabolic and transcriptomic analyses reveal different metabolite biosynthesis profiles between leaf buds and mature leaves in *Ziziphus jujuba* mill. *Food Chem* **347**:129005 https://doi.org/10.1016/j.foodchem.2021.129005 | PubMed

Li T, Guo J, Hu G, Cao F, Su H, Shen M, Wang H, You M, Liu Y, Gurr GM, *et al.* (2024b) Zinc finger proteins facilitate adaptation of a global insect pest to climate change. *BMC Biol* **22**:303 https://doi.org/10.1186/s12915-024-02109-3 | PubMed

Li Y, Song H, Xie L, Tang X, Jiang Y, Yao Y, Peng X, Cui J, Zhou Z, Xu J (2024c) Surviving high temperatures: The crucial role of vesicular inhibitory amino acid transporter in Asian honeybee, *Apis cerana*. *Int J Biol Macromol* **279**:135276 https://doi.org/10.1016/j.ijbiomac.2024.135276 | PubMed

Liu SS, Chen FZ, Zalucki MP (2002) Development and survival of the diamondback moth (Lepidoptera: Plutellidae) at constant and alternating temperatures. *Environ Entomol* **31**:221-231 https://doi.org/10.1603/0046-225x-31.2.221

Mallard F, Nolte V, Tobler R, Kapun M, Schlotterer C (2018) A simple genetic basis of adaptation to a novel thermal environment results in complex metabolic rewiring in *Drosophila*. *Genome Biol* **19**:119 https://doi.org/10.1186/s13059-018-1503-4 | PubMed

McCulloch GA, Waters JM (2022) Rapid adaptation in a fastCchanging world: Emerging insights from insect genomics. *Glob Change Biol* **29**:943-954 https://doi.org/10.1111/gcb.16512 | PubMed

McKean IJW, Sadler JC, Cuetos A, Frese A, Humphreys LD, Grogan G, Hoskisson PA, Burley GA (2019) S-adenosyl methionine cofactor modifications enhance the biocatalytic repertoire of small molecule c-alkylation. *Angew Chem Int Ed Engl* **58**:17583-17588 https://doi.org/10.1002/anie.201908681 | PubMed

Mondola P, Damiano S, Sasso A, Santillo M (2016) The Cu, Zn superoxide dismutase: not only a dismutase enzyme. *Front Physiol* **7**:594 https://doi.org/10.3389/fphys.2016.00594 | PubMed

Ni P, Nie F, Zhong Z, Xu J, Huang N, Zhang J, Zhao H, Zou Y, Huang Y, Li J, *et al.* (2023) DNA 5-methylcytosine detection and methylation phasing using PacBio circular consensus sequencing. *Nat Commun* **14**:4054 https://doi.org/10.1038/s41467-023-39784-9 | PubMed

Nobeli I, Favia AD, Thornton JM (2009) Protein promiscuity and its implications for biotechnology. *Nat Biotechnol* **27**:157-167 https://doi.org/10.1038/nbt1519 | PubMed

Outhwaite CL, McCann P, Newbold T (2022) Agriculture and climate change are reshaping insect biodiversity worldwide. *Nature* **605**:97-102 https://doi.org/10.1038/s41586-022-04644-x | PubMed

Patsch D, Schwander T, Voss M, Schaub D, Hüppi S, Eichenberger M, Stockinger P, Schelbert L, Giger S, Peccati F, *et al.* (2024) Enriching productive mutational paths accelerates enzyme evolution. *Nat Chem Biol* **20**:1662-1669 https://doi.org/10.1038/s41589-024-01712-3 | PubMed

Quan PQ, Guo PL, He J, Liu XD (2024) Heat-stress memory enhances the acclimation of a migratory insect pest to global warming. *Mol Ecol* **33**:e17493 https://doi.org/10.1111/mec.17493 | PubMed

Reynolds JA (2017) Epigenetic influences on Diapause. In: Verlinden H (Ed). *Advances in Insect Physiology* **53** Academic Press. pp. 115-144

Rommelaere S, Boquete JP, Piton J, Kondo S, Lemaitre B (2019) The exchangeable apolipoprotein Nplp2 sustains lipid flow and heat acclimation in *Drosophila*. *Cell Rep* **27**:886-899 https://doi.org/10.1016/j.celrep.2019.03.074 | PubMed

Schoville SD, Farrand Z, Kavanaugh DH, Veire B, Weng YM (2024) Environmental stress responses and adaptive evolution in the alpine ground beetle *Nebria vandykei*. *Biol J Linn Soc* **141**:51-70 https://doi.org/10.1093/biolinnean/blad093

Sheng Y, Abreu IA, Cabelli DE, Maroney MJ, Miller AF, Teixeira M, Valentine JS (2014) Superoxide dismutases and superoxide reductases. *Chem Rev* **114**:3854-3918 https://doi.org/10.1021/cr4005296 | PubMed

Sheng Y, Durazo A, Schumacher M, Gralla EB, Cascio D, Cabelli DE, Valentine JS (2013) Tetramerization reinforces the dimer interface of MnSOD. *PLoS One* **8**:e62446 https://doi.org/10.1371/journal.pone.0062446 | PubMed

Sherpa S, Tutagata J, Gaude T, Laporte F, Kasai S, Ishak IH, Guo X, Shin J, Boyer S, Marcombe S, *et al.* (2022) Genomic shifts, phenotypic clines, and fitness costs associated with cold tolerance in the Asian tiger mosquito. *Mol Biol Evol* **39**:104 https://doi.org/10.1093/molbev/msac104 | PubMed

Stroud H, Song Q, Guan X, Chen ZJ (2015) Dynamic roles for small RNAs and DNA methylation during ovule and fiber development in allotetraploid cotton. *PLoS Genet* **11**:1005724 https://doi.org/10.1371/journal.pgen.1005724 | PubMed

Tigano A, Colella JP, MacManes MD (2020) Comparative and population genomics approaches reveal the basis of adaptation to deserts in a small rodent. *Mol Ecol* **29**:1300-1314 https://doi.org/10.1111/mec.15401 | PubMed

Wang P, Shi S, Ma J, Song H, Zhang Y, Gao C, Zhao C, Zhao S, Hou L, Lopez-Baltazar J, *et al.* (2018) Global methylome and gene expression analysis during early Peanut pod development. *BMC Plant Biol* **18**:352 https://doi.org/10.1186/s12870-018-1546-4 | PubMed

Wang Y, Huang Y, Xu X, Liu Z, Li J, Zhan X, Yang G, You M, You S (2020) CRISPR/Cas9Cbased functional analysis of yellow gene in the diamondback moth, *Plutella xylostella*. *Insect Sci* **28**:1504-1509 https://doi.org/10.1111/1744-7917.12870

Wang Z, Receveur JP, Pu J, Cong H, Richards C, Liang M, Chung H (2022) Desiccation resistance differences in *Drosophila* species can be largely explained by variations in cuticular hydrocarbons. *eLife* **11**:80859 https://doi.org/10.7554/elife.80859 | PubMed

You M, Ke F, You S, Wu Z, Liu Q, He W, Baxter SW, Yuchi Z, Vasseur L, Gurr GM (2020) Variation among 532 genomes unveils the origin and evolutionary history of a global insect herbivore. *Nat Commun* **11**:1-8 https://doi.org/10.1038/s41467-020-16178-9 | PubMed

You M, Yue Z, He W, Yang X, Yang G, Xie M, Zhan D, Baxter SW, Vasseur L, Gurr GM, *et al.* (2013) A heterozygous moth genome provides insights into herbivory and detoxification. *Nat Genet* **45**:220-225 https://doi.org/10.1038/ng.2524 | PubMed

You S, Lei G, Zhou H, Li J, Chen S, Huang J, Vasseur L, Gurr GM, You M, Chen Y (2024) Thermal acclimation uncovers a simple genetic basis of adaptation to high temperature in a cosmopolitan pest. *iScience* **27**:109242 https://doi.org/10.1016/j.isci.2024.109242 | PubMed

Zhou H, Lei G, Chen Y, You M, You S (2022) *PxTret1-like* affects the temperature adaptability of a cosmopolitan pest by altering trehalose tissue distribution. *Int J Mol Sci* **23**:9019 https://doi.org/10.3390/ijms23169019 | PubMed

Zhou H, Lei G, Li Y, Chen P, Liu Z, Li C, Li B (2024) Novel regulation pathway of eclosion hormones in *Tribolium castaneum* by distinct transcription factors through the initiation of 20-hydroxyecdysone. *J Biol Chem* **300**:107898 https://doi.org/10.1016/j.jbc.2024.107898 | PubMed

Gaoke Lei (2025) transcriptome sequencing of Plutella xylostella. the Genome Sequence Archive at the National Genomics Data Center. ID CRA024611 https://ngdc.cncb.ac.cn/gsa

Gaoke Lei (2025) metabolomics of Plutella xylostella. the Genome Sequence Archive at the National Genomics Data Center. ID OMIX009807 https://ngdc.cncb.ac.cn/omix/preview/kkl093nl

Gaoke Lei (2025) metabolomics of diamondback moth. the Genome Sequence Archive at the National Genomics Data Center. ID OMIX009846 https://ngdc.cncb.ac.cn/omix/preview/gXwZCXMI

Peer reviews

Reviewer #1 (Public review):

Summary:

In this manuscript, Lei and co-workers aim to uncover the genetic underpinnings of thermal adaptation across three strains of the diamondback moth (Plutella xylostella) through experimental evolution over three years under three different thermal regimes. They identify systematic differences in trait responses (e.g., survival, fecundity), metabolic profiles, gene expression, and in the amino acid sequence of the PxSODC gene, among others. These results suggest that the diamondback moth has a strong potential for rapid physiological adaptation to different thermal regimes. Overall, this is a comprehensive and generally well-executed study that addresses an important question in the face of ongoing climate change.

Strengths:

The authors employ multiple approaches to identify signatures of thermal adaptation across the three strains, such as trait performance comparisons, metabolomics, transcriptomics, and amino acid sequence comparisons. All these different angles form a convincing picture of the underlying factors that underpin thermal adaptation in this experimental system. The manuscript is also generally well written and easy to understand.

https://doi.org/10.7554/eLife.110352.2.sa2

Reviewer #2 (Public review):

Summary:

In this paper, the authors set out to better understand the genetic mechanisms underlying thermal adaptation in insects. They experimentally evolved diamondback moth (Plutella xylostella) populations - a pest species with a wide distribution - under both hot (12h:12h 32{degree sign}C/27{degree sign}C) and cold (15{degree sign}C/10{degree sign}C) thermal conditions, and conducted phenotypic assays and metabolic and transcriptomic profiling to analyze how populations changed to deal with this thermal stress compared to the nonevolved ancestral population (constant 26{degree sign}C). Phenotypic assays showed that evolved hot populations had increased survival at high temperatures (42-43{degree sign}C) while evolved cold populations had lower freezing points compared to the ancestral population. When measured at the constant 26{degree sign}C conditions, metabolic and transcriptomic profiles of 3rd instar larvae from the evolved population were distinctive from the ancestral population, with a set of overlapping metabolic and transcriptomic pathways that were significantly differentially expressed in both hot and cold evolved populations compared to the ancestral. The authors narrowed down this set of candidate genes further by focusing on genes with high expression levels overall, whose expression profile was correlated with differentially expressed metabolites, and that contained mutants in both hot and cold strains. From this set, they chose the PxSODC gene for further functional validation, as it has previously been shown to be involved in the response of insects to abiotic stress with its antioxidative role in cellular defense. At the constant 26{degree sign}C, this gene showed lower expression across development in evolved strains compared to the ancestral population, while it showed similar expression patterns under thermal stress. Knockdown of PxSODC resulted in decreased survival rates at high temperatures and higher freezing points compared to the ancestral population. Based on this validation, the authors hypothesize that the non-synonymous mutation in the PxSODC gene that they found in the cold and hot evolved populations might alter the conformation of the PxSODC protein, increasing enzyme capacity. Their experimental evolution experiment furthermore indicates

the capacity of the pest species, the diamondback moth, to adapt to a wide range of temperatures, providing insights into its capacity for global dispersal.

Strengths:

(1) The authors did a tremendous amount of work to characterize the mechanisms underlying thermal adaptation in the diamondback moth, artificially selecting populations for three years in the lab and characterizing how they evolved as a result at different biological levels: from phenotypes in different life stages, to larval metabolites and gene transcription, to functionally validating how one of the resulting gene candidates influences the capacity to deal with thermal stress.

(2) The paper identifies and provides further evidence for candidate genetic mechanisms that might be particularly important for thermal adaptation in insects, including lipid metabolism, oxidoreductase activity, and DNA methylation. It is furthermore interesting that the authors found similar mechanisms to be involved in both the adaptation to cold and hot environments. Their functional validation of some of the genes involved in these mechanisms is very useful to understand how these genes might be causally involved in insect thermal adaptation.

(3) The paper also has applied value: the diamondback moth is a pest species with a wide distribution, so understanding its adaptive capacity to different thermal environments is important for predicting the prevalence and potential further range expansion of this species under future climate change.

https://doi.org/10.7554/eLife.110352.2.sa1

Author response:

The following is the authors' response to the original reviews.

> ***eLife Assessment***
>
> *This important study deepens our understanding of how populations of a given species may diverge in their molecular and physiological patterns as a result of adaptation to different thermal regimes. By approaching this question from multiple directions, the authors provide solid evidence for adaptive changes in three strains of the diamondback moth after only three years of experimental evolution, and support the causal involvement of the PxSODC gene in thermal adaptation to both cold and hot temperatures. This work would benefit from more sophisticated phylogenetic analyses, better statistical support, and a more detailed discussion of the differences in the three strains at the pathway level.*

We sincerely thank the editors for this positive and constructive assessment. In the revised manuscript, we have addressed the highlighted points by: (1) re-inferring the phylogenetic tree of the *PxSODC* gene using a model-based Maximum Likelihood method (IQ-TREE) to ensure a robust evolutionary analysis; (2) substantially expanding the description of our statistical methods across all data types to ensure reproducibility and clarify multiple-testing corrections; and (3) adding a more detailed discussion of the pathway-level differences between the hot and cold strains, particularly integrating how their distinct transcriptomic responses align with their shared metabolic adjustments and phenotypic traits.

> ***Reviewer #1 (Public review):***
>
> *(1) The authors identify pathways that are enriched in different strain comparisons (Figure 3E), but do not provide a detailed interpretation of these results. It would be*

> *great if the authors could explain in more detail how the physiological processes of a cold-adapted strain of this species may differ from those of a warmer-adapted strain.*

We agree. We have addressed this by directly integrating our pathway enrichment results (Figure 3E) with the observed life-history phenotypes (concurrently addressing Reviewer 2's Comment 36a). We expanded the Discussion to explain that while both strains share convergent adjustments in core pathways (e.g., lipid metabolism for energy reallocation), their specific physiological strategies differ. The cold-adapted strain relies on broader transcriptional reprogramming to maintain homeostasis and support extended longevity/cold hardiness, whereas the hot-adapted strain utilizes broader metabolic rewiring to actively fuel its accelerated development and higher fecundity.

> *(2) The authors reconstruct a phylogenetic tree of the PxSODC gene using the neighbor-joining algorithm. The limitations of this algorithm have been known for many years now, especially for sequences separated by long evolutionary distances. According to Wang et al. (2016), the last common ancestor of the species shown in Figure S4C occurred 392-350 million years ago. Given this, I would strongly recommend that the authors infer a phylogenetic tree using model-based methods, such as those implemented in RAxML-NG or IQ-TREE. Also, in the absence of a valid outgroup sequence, I would show the gene tree as unrooted or rooted based on the corresponding species tree.*

Agree. We have re-inferred the phylogenetic tree of the *PxSODC* gene using the model-based Maximum Likelihood (ML) method implemented in IQ-TREE. As recommended, in the absence of a valid outgroup sequence, the revised tree is now presented as unrooted. Supplemental Figure S4C (Figure 5-figure supplement 1C) and the corresponding text in the manuscript have been updated.

> *(3) There is a key piece of the puzzle that is currently missing: the structural mechanism behind the mutational effects described in this study (e.g., Figure 5). The authors could leverage AlphaFold to generate structural models of different mutants and conduct molecular dynamics simulations to examine their conformational dynamics.*

We thank the reviewer for this excellent suggestion. We generated AlphaFold structural models of the wild-type (WT) and mutant (MU) PxSODC proteins and conducted 100 ns molecular dynamics (MD) simulations using GROMACS 2022.3 at three physiologically relevant temperatures: 15°C (cold stress), 26°C (favorable baseline), and 32°C (heat stress). Using 26°C as the physiological baseline, three key structural parameters support enhanced thermostability of the mutant protein (Figure 5–figure supplement 3). First, RMSD analysis revealed that under heat stress (32°C), the WT underwent severe conformational drift (RMSD increased from the 26°C baseline of 1.62 to 2.49, an increase of 0.87), while MU remained remarkably stable (from 1.59 to 1.66, an increase of only 0.07). Second, MU possessed a significantly more compact structure, with lower SASA values at 15°C (118.39 vs. 127.29 nm^2) and 26°C (113.82 vs. 125.61 nm^2), indicating optimized hydrophobic core packing. Third, the intramolecular hydrogen bond network of MU demonstrated dual stress resistance: under cold stress, MU actively increased hydrogen bonds from its baseline (113→119), whereas WT lost bonds (117→112); under heat stress, MU fully maintained its bond count (113→113). These results provide a direct structural mechanism for the enhanced catalytic efficiency of the mutant SOD at lower expression levels.

> ***Reviewer #1 (Recommendations for the authors):***
>
> *(4) The experimental evolution component of this study is described in the text as lasting for three years. It would help if the number of generations per strain were also reported.*

We have added the number of generations per strain. Over the three-year period, the hot

strain completed ~75 generations and the cold strain ~15 generations. The ancestral strain was continuously maintained at 26°C throughout this period. The revised text has been updated in both the Introduction and Materials and Methods.

> *(5) In Figure 3B: There is a typo in the word "Statistics".*

Corrected. The typo in "Statistics" in Figure 3B has been fixed.

> *(6) In Figure 3D: "CS" appears twice.*

Corrected. The duplicated "CS" label in Figure 3D has been replaced with the correct label.

> *(7) Figure 4: This is not accessible to colorblind readers, who will clearly not be able to tell each color apart. As a non-colorblind person, I, too, have trouble figuring out which color label in panel B corresponds to which color in panel A. For example, I do not know off the top of my head how 'blue' differs from 'midnightblue', 'royalblue', or 'skyblue'. I recommend that the authors replace colors with identifiers, such as 'g1' for group 1 and so on.*

We appreciate this suggestion. We have replaced all color-based module labels with alphanumeric identifiers (M1, M2, M3, etc.) and added a corresponding legend. The main text and supplementary materials have been updated accordingly.

> *(8) Lines 246-247: "Its secondary structure mainly consisted of strands, helices and coils." This sentence is redundant. These three are the only possible secondary structural elements, according to most bioinformatics tools such as PSIPRED, which the authors used. This sentence would be more useful if the authors could report the percentage breakdown of each secondary structural element.*

We have removed the redundant sentence and updated the text to report the specific percentage breakdown of the secondary structural elements based on our PSIPRED predictions (approximately 55.24% random coils, 16.19% alpha helices, and 28.57% extended strands). The revised text has been updated in the Results section.

> *(9) Lines 260-261: "This suggests that the PxSODC gene can alter its expression pattern and function in response to environmental change...". I find this sentence a bit imprecise. Would it not be more precise to mention that the expression of this gene is regulated by temperature triggers?*

We agree that the original phrasing was imprecise. We have revised the sentence in the manuscript to state: "This suggests that the expression of the *PxSODC* gene is regulated by temperature triggers, and its altered function contributes to temperature-adaptive evolution in *P. xylostella*."

> *(10) The data points in Figures S1 and S7 are very small and hard to tell apart without zooming in a lot. Perhaps the authors could change the orientation of those pages to landscape and increase the size of the figures.*

Done. We have changed the orientation of Supplemental Figures S1 (Figure 1-figure supplement 1) and S7 (Figure 5-figure supplement 4) to landscape and increased the size of the figures and individual data points to improve visibility.

> *(11) In Figure S2, the panel labeled as 'C' should be 'B' (based on the caption) and vice versa.*

Corrected. The panel labels 'B' and 'C' in Supplemental Figure S2 (Figure 2-figure supplement 1) have been swapped. The Supplementary Materials have been updated accordingly.

> ***Reviewer #2 (Public review):***
>
> *(1) The paper in its current form is hard to digest and would benefit from improved clarification of the storyline, as well as a tighter integration between the phenotypic, omics, and functional validation data. Currently, it is not always clear what the relevance is of all the reported results, nor why certain decisions were made, or how all the different methods the authors used fit together. For example, the authors functionally validated a second gene, PxDnmt1, but it is unclear why this particular gene was chosen, nor how it relates to their selection regimes when looking at the results obtained with the phenotyping and omics data collection. Seeing how much work the authors did, this makes the paper overwhelming and difficult to read.*

We sincerely appreciate this constructive feedback. In the revised manuscript, we have made significant structural revisions to improve the storyline and logical flow. We have streamlined the Results section (moving extensive descriptive data like life table curves and detailed metabolomics of mutant strains to the Appendix 1-3) to focus on the key findings. Furthermore, we have clarified the logical transitions between experiments. For instance, regarding the choice to validate *PxDnmt1*, we now explicitly explain in the Results that our untargeted metabolomic analysis of the *PxSODC* mutant strains revealed consistent alterations in 5-hydroxymethyluracil (involved in DNA demethylation) and 5'-deoxyadenosine (a precursor to the primary methyl donor S-adenosylmethionine) across all developmental stages. This specific metabolic signature provided a strong, data-driven hypothesis linking *PxSODC* function to epigenetic regulation via DNA methylation, prompting us to functionally validate *PxDnmt1*. By explicitly stating these rationales, the narrative is now much clearer and cohesive.

> *(2) The authors at times stretch their results too far, as the ecological relevance of their study design and results is not clear, limiting the generalizability and value of the results for understanding species' adaptive potential under climate change. For example, the selection regimes used present the minimum and maximum known temperatures at which the species can survive and develop, but it is unclear how the temperatures relate to the natural environment of the source population, to what extent wild populations might experience these temperatures, and whether they would experience them at the extended duration used (12h at max/min temperature). Moreover, I wonder whether the comparisons made would identify the genes that matter under natural conditions, as unevolved populations were kept under constant conditions compared to 12h:12h temperature regimes for the evolved populations, and the metabolic and transcriptomic profiling was done under a constant favorable 26°C rather than under thermal stress in a, as far as I can tell, randomly chosen life stage (larval stage).*

We appreciate the reviewer raising these important points regarding ecological relevance and experimental design. In the revised manuscript, we have added context and acknowledged these limitations in the Methods and Discussion sections. First, regarding ecological relevance: The source population is from Fuzhou, a subtropical region where summer high temperatures frequently exceed 32°C and winter lows can drop below 10°C, making our selection temperatures ecologically relevant extremes for this population. The 12h:12h cycling temperatures were designed to simulate severe but natural diurnal fluctuations.

Second, regarding constant control vs. cycling regimes: The constant 26°C represents the established optimal developmental temperature and standard laboratory condition for *P. xylostella*. We acknowledge that comparing cycling selection regimes against a constant control might conflate adaptation to absolute temperature extremes with adaptation to thermal fluctuation itself. We have added this as a caveat in the Discussion. Third, regarding omics profiling conditions: The transcriptomic and metabolomic profiling was conducted

under common garden conditions (26°C) specifically to identify constitutive, genetically fixed adaptations resulting from evolutionary selection, rather than immediate physiological plasticity under stress. We have clarified these rationales in the text.

> *(3) The paper in its current form does not adequately describe the statistical analyses underlying the results, nor do the authors share their code, making it very hard to judge whether the analyses used are appropriate and the results trustworthy. I have concerns about the inappropriate use of t-tests, the lack of correcting for confounding variables, and the need for multiple testing corrections.*

We sincerely appreciate this concern. In the revised manuscript, we have made substantial improvements to the description of statistical analyses throughout the Methods section:

(1) Statistical methods for each data type are now described separately and in detail, specifying the tests used, the number and type of comparisons, and sample sizes.

(2) For metabolomic data, we have clarified that FDR correction was applied alongside multi-criteria thresholds ($|\log_2\text{Fold Change}| \geq 1$, VIP ≥ 1, FDR < 0.05). For transcriptomic data, FDR correction (Benjamini and Hochberg, 1995) was applied via DESeq2.

(3) For WGCNA, we have specified the total number of correlation tests (29 modules × 30 metabolites = 870) and the stringent dual threshold ($|r| > 0.8$, $P < 0.05$) used to control for false positives, following standard practice.

(4) For life table parameters, the paired bootstrap method with 100,000 replications was used for all pairwise comparisons among strains.

(5) For all other experimental data (qRT-PCR, SOD activity, O_2^- levels, survival rates, supercooling/freezing points, etc.), we have specified that t-tests were used only for two-group comparisons, while one-way ANOVA with Tukey's or Tamhane's T2 test was used for three or more groups, with non-parametric alternatives applied when normality assumptions were not met.

(6) The raw data have been deposited in public repositories (see Data availability), and all statistical procedures are now described in sufficient detail to enable independent reproduction of the results.

> ***Reviewer #2 (Recommendations for the authors):***
>
> *Title*
>
> *(4) I don't feel the title adequately captures the work, I would instead of 'adaptive evolution' use 'experimental evolution' and I would not use the word 'underpins' but instead 'indicates', as it is not clear from your work whether the adaptations to the lab conditions you used would be ecologically relevant nor whether they are involved in thermal adaptation in wild populations.*

Accepted. The title has been revised to: “Experimental evolution to thermal stress indicates climate resilience in a cosmopolitan arthropod.”

> *Abstract*
>
> *(5a) Please add the phenotype results to the abstract.*

We have added key phenotype results to the abstract. The revised text now reads: “The hot strain showed accelerated development, higher fecundity, and increased survival under extreme heat, while the cold strain exhibited lower supercooling and freezing points, indicating enhanced cold hardiness.”

> *(6b) The Abstract doesn't really detail the answer to your research question yet: so what insights into the genetic mechanisms underlying thermal adaptation did you gain that are novel?*

We agree. We have revised the Abstract to explicitly highlight the novel genetic and molecular mechanisms we discovered. Specifically, we now detail that thermal adaptation is driven by a coordinated mutational, metabolic, and epigenetic (1) an energy-efficient genetic mechanism where non-synonymous mutations in *PxSODC* enhance superoxide scavenging efficiency, enabling effective oxidative stress management at lower gene expression levels; (2) convergent metabolic adjustments, notably a reduction in lipid metabolism to conserve energy; and (3) epigenetic regulation of thermal tolerance via DNA methylation. The revised text has been updated in the Abstract accordingly.

> *(7c) Line 3: replace 'ectotherms' with 'arthropods' to match the title?*

Done. “Terrestrial ectotherms” has been replaced with “terrestrial arthropods” in the abstract.

> *(8d) Line 9: replace 'demographic' with 'life history'?*

Done. “Demographic” has been replaced with “life history” in the abstract.

> *Introduction*
>
> *(9a) The storyline is a bit unclear. Do you want to focus on the increased threat from insect pests under climate change or on the threat of climate change on insect persistence? Please pick one and adapt your storyline accordingly. I would suggest focusing on the first and talking more about the range extension of pest species under climate change (which would also require adaptation to cold extremes).*

We agree and have refocused the Introduction on the increased threat from insect pests under climate change, emphasizing that range expansion into new regions requires adaptation to both heat and cold extremes. Both the first and second paragraphs have been revised accordingly.

> *(10b) Line 31-33: What do you mean by 'shows a positive relationship between the thermal tolerance range and the level of climatic variability'? Are they able to tolerate a larger range of temperatures?*

This sentence has been revised as part of the restructured Introduction, which now focuses on the range expansion of pest species under climate change. The revised text reads: “Such range expansion requires adaptation not only to warmer conditions in existing habitats but also to cold extremes encountered during colonization of higher latitudes or elevations (Harvey et al., 2020).”

> *(11c) Line 33-35: Is this information relevant here?*

Agreed. This sentence has been removed as part of the restructured Introduction, which now focuses on the threat of pest range expansion under climate change.

> *(12d) Line 55-56: What exactly do we not know yet about the mechanisms that enable thermal adaptation that you aim to fill in this paper? Please rephrase your knowledge gap to be more concrete (e.g., "but we do not yet know how...").*

We have rephrased the knowledge gap to be more concrete and aligned with the revised storyline. The revised text now reads: "...we do not yet know how long-term thermal selection drives coordinated changes across gene function, metabolic networks, and life history traits to enable thermal adaptation and range expansion in pest species."

> *(13e) Line 57: Also, here, the storyline is unclear. Why did you use the diamondback moth as your model species? You provide many different reasons, but it would help if you emphasized one reason that is in line with whichever storyline you want to focus on: is it because it is an insect pest that can tolerate a wide range of temperatures?*

We have streamlined this paragraph to focus on the primary rationale: *P. xylostella* is a globally distributed pest that thrives across a wide range of thermal environments, making it an ideal model for studying the genetic mechanisms of thermal adaptation. Supporting details on genomic resources are retained briefly as they enable the multi-omics approach used in this study.

> *(14f) Line 65: Demonstrated how? Please give a short summary of the evidence for their genetic capacity to tolerate future climates.*

We have added a brief summary of the evidence. Specifically, genome-wide SNP analysis of field populations from 114 locations across diverse biogeographical zones revealed climate-adaptive genetic variability, indicating that *P. xylostella* can tolerate projected future climates in most regions (Chen et al., 2021).

> *(15g) Line 72: What does 'Age-stage' mean? Should it read 'Aged-staged'?*

"Age-stage, two-sex life table" is an established demographic method developed by Chi (1988) that simultaneously accounts for both age and developmental stage in both sexes. This is a standard term in the field (Chi et al., 2020), so we have retained the original wording but added a brief clarification upon first use.

> *(16h) Line 78-80: This needs a bit more explanation. Why does an increased ability to scavenge superoxide anions affect adaptability under extreme temperature environments?*

We have added a brief explanation. Extreme temperatures induce oxidative stress by elevating intracellular reactive oxygen species (ROS), including superoxide anions, which can damage cellular structures. Enhanced scavenging capacity thus helps maintain cellular homeostasis under thermal stress.

> *(i) Line 82-86: Please be more precise. What novel insights did you gain about the genetic mechanisms underlying thermal adaptation?*

We have revised this sentence to more precisely summarize the novel insights, encompassing both the multi-omics findings and the functional validation of *PxSODC*.

> *Results*
>
> *(18a) The results section is very long and presents an overload of information at the moment, overwhelming the reader. Consider moving some sections to the Supplements (for example, a large part of the phenotypic data that cannot be linked to the omics data and the metabolic profiling of the mutant strains) or leave them out of the paper altogether.*

We agree that the Results section was too dense. We have streamlined it by moving the following content to the Supplementary Materials:

(1) Detailed age-stage survival and fecundity curve data for the ancestral, hot and cold strains (Supplementary Text S1).

(2) Detailed life table analysis of the *PxSODC* mutant strains (Supplementary Text S2).

(3) Detailed untargeted metabolomic profiling of the SODC-MU mutant strains across developmental stages (Supplementary Text S3).

The main text now retains only the key life history comparisons, extreme temperature tolerance results, omics-based evidence linking transcriptomics and metabolomics, functional validation of *PxSODC*, and the DNA methylation findings, with brief summaries and cross-references to the Supplements for supporting details.

> *(19b) Please also provide the effect sizes for the different effects you report, for example, how many degrees difference was there between ancestral and cold strains in the supercooling/freezing points, and what was the variation?*

We have added specific effect sizes (mean ± SEM and between-group differences) for all key comparisons throughout the Results section, including preadult duration, stage-specific survival rates under extreme heat, supercooling/freezing points, and SODC-MU mutant strain comparisons. For example, the supercooling points of CS pupae (-23.99 ± 0.18°C) were 0.90°C lower than AS (-23.09 ± 0.26°C), and the freezing points were 2.66°C lower (-14.24 ± 0.61°C vs. -11.58 ± 0.52°C). Please refer to the revised manuscript for all updated values.

> *(20c) Line 93-94: "Intrinsic and finite rate of increase" of what?*

Clarified. These are population growth parameters. The revised text now specifies “intrinsic rate of increase (r) and finite rate of increase (λ) of the population.”

> *(21d) Line 98-99: Please start the paragraph with this summary of the results and then further detail them.*

We have restructured this paragraph by moving the summary sentence to the beginning, followed by the supporting details.

> *(22e) Line 100-109: Why did you look at daily survival and fecundity rates? Please add why this is relevant.*

As part of the overall streamlining of the Results section, this paragraph on detailed age-stage survival and fecundity curves has been moved to Supplementary Text S1. A brief justification for their relevance has been added there, noting that these curves capture stage-specific variation in survival and fecundity that summary life table parameters alone may obscure.

> *(23f) Line 106: What do HS, AS, and CS stand for? And please provide the statistics for comparison of daily survival rates between the strains.*

We have defined the abbreviations (HS = hot strain, AS = ancestral strain, CS = cold strain) at their first appearance in the Results section. This paragraph on daily survival and fecundity has been moved to Supplementary Text S1, where the abbreviations are also defined. The survival rates reported are the maximum daily survival rates derived from the age-stage specific survival rate curves (s_{xj}), and the statistical comparisons among strains are presented in Supplemental Table S1.

> *(24g) Line 144-146: Why are these differential metabolites likely to play a crucial role?*

We agree this statement was speculative. It has been removed from the revised manuscript.

> *(25h) Line 159-161: Why is a reduction of lipid metabolites evidence for adaptive evolution?*

We have revised this sentence to clarify the reasoning. The reduction in lipid metabolites in both independently evolved hot and cold strains suggests a convergent metabolic response, indicating that lipid metabolism adjustment is a shared adaptive strategy rather than a random change.

> *(26i) Line 184-185: It is difficult to judge from Figure 3E the extent of overlap in KEGG pathways between the hot and cold strains. Can you adjust the figure to emphasize that overlap more?*

Agree. To intuitively emphasize the extent of overlap in KEGG pathways between the hot and cold strains, we have completely redesigned Figure 3E. Instead of presenting two separate panels with unaligned vertical axes, we have consolidated the data into a single back-to-back (mirrored) bar chart with a shared central y-axis.

> *(27j) Line 211: Not only the red module, but also the blue and green module correlates with many of the shared differential metabolites.*

We agree. We have revised the text to acknowledge that the blue and green modules also showed strong correlations with shared differential metabolites, while noting that the red module had the highest number of significantly correlated metabolites and was therefore selected for further analysis.

> *(28k) Line 215: I would rephrase this as genes being interesting candidates for being involved in thermal adaptation or 'seem to be important for the adaptation of…', as you don't know from these results whether these genes play a critical regulatory role.*

Agreed. We have toned down the language to reflect the correlative nature of these results.

> *(29l) Line 233: Do you mean that you further analyzed 15 genes of the 79 identified candidate genes in the previous paragraph?*

Yes, exactly. From the 79 candidate genes, we selected 15 that were both annotated in the genome and had high expression levels (FPKM > 10) for further analysis. We have clarified this in the revised manuscript.

> *(30m) Line 238: What does SOD stand for?*

We have spelled out the abbreviation upon first use in this section.

> *(31n) Line 254-255: Please provide the stats for this result.*

We have added the specific allele frequencies for each strain. The Leu194-Met194 mutation frequency was determined by direct sequencing of 10 individuals per strain, and the frequencies are now reported in the revised text.

> *(32o) Line 303-304: How did you test for enhanced stability to temperature fluctuations? And enhanced compared to what?*

This observation was based on the survival rate data in Figure 5C, where mutant pupae at 43°C showed no significant difference from the ancestral strain, whereas other life stages (eggs, larvae, adults) at 42°C showed significantly reduced survival in the mutant strains. We have revised the text to clarify the comparison.

> *(33p) Line 324-326: Why do decreased expression levels demonstrate increased O_2^- scavenging capacity? And why is that beneficial for adaptation to thermal stress? Please*

> *explain.*

We have revised this sentence to clarify the logic. The non-synonymous mutations in the hot and cold strains likely alter the protein conformation of SOD enzymes, increasing their catalytic efficiency per molecule. This allows effective O_2^- scavenging at lower expression levels, which is energetically favorable under thermal stress where energy conservation is critical for survival.

> *(34q) Line 404-406: I'm confused. Is there a direct link between the gene you knocked out here and the results you presented up until now? How do the reduced levels of 5-methylcytosine relate to the metabolite results you present at the beginning of the paragraph, other than that both could be involved in DNA methylation?*

We have revised this paragraph to clarify the logical chain. Among the three metabolites consistently altered across all developmental stages in the SODC-MU strains, 5-hydroxymethyluracil is involved in dynamic DNA demethylation and 5'-deoxyadenosine is a precursor to S-adenosylmethionine (the methyl donor for DNA methylation). This suggested a link between *PxSODC* deletion and DNA methylation. To test this, we examined *PxDnmt1* expression and activity in the thermally adapted strains and found both were significantly reduced. We then used RNAi to silence *PxDnmt1* and confirmed that reduced DNA methylation (lower 5-mC levels) directly impaired thermal tolerance. Thus the connection is: *PxSODC* deletion → altered methylation-related metabolites → reduced DNA methyltransferase activity → decreased thermal tolerance.

> *(35r) Line 410: Saying that your knockdown of a gene that did not directly pop up in any of your other analyses confirms that DNA methyltransferase is associated with the response to thermal selection is a stretch. Please rephrase.*

We agree this was overstated. We have toned down the language to reflect that the RNAi results provide preliminary evidence for a potential role of DNA methylation in thermal tolerance, rather than confirmation.

> *Discussion*
>
> *(36a) The phenotype data are currently not discussed at all. Please add it to the discussion and try to integrate it more with the omics data you collected.*

We agree. To provide a cohesive narrative and avoid redundancy, we have addressed this comment in conjunction with our pathway interpretation (please see our response to Reviewer 1, Comment 1). In the revised Discussion, we explicitly integrated our specific phenotypic findings (e.g., accelerated development, increased fecundity, and heat survival in the hot strain; prolonged lifespan and lowered supercooling points in the cold strain) with the distinct transcriptomic and metabolomic profiles. This integration demonstrates how molecular and metabolic rewiring directly underpins the divergent life-history traits without engaging in unwarranted speculation.

> *(37b) Line 433-434: I don't think this adequately represents the relevance of your particular study. I would suggest changing it to be more in line with the storyline of understanding the capacity for global dispersal in insect pests under climate change.*

We agree. We have revised this sentence to align with the storyline of pest range expansion under climate change.

> *(38c) Line 476: This is a very odd statement; don't all species' genomes have genes encoding proteins involved in thermal adaptation? The reference also doesn't seem to be appropriate. I would suggest deleting this sentence.*

Agreed. This sentence has been removed.

> *(39d) Line 483: Please write out SOD the first time you use it in a new section.*

Done. SOD has been spelled out at its first use in the Discussion.

> *(40e) Line 544-548: This is a bit too specific to be the last sentence of the discussion. Try to formulate it more broadly in terms of what future research should focus on in general, not just your specific research.*

We agree. We have broadened the final sentence to address future research directions more generally.

> *Figures*
>
> *(41a) Figure 1A: I don't think t-tests are appropriate here since you are not simply comparing two treatments, but testing for the effects of 5-6 different temperatures. And how did you correct for replicate populations in your analysis?*

Clarified. In Figure 1A, our comparisons are independent pairwise tests between exactly two strains (HS vs. AS) at each specific temperature and time point, making t-tests statistically appropriate. We were not testing for a continuous effect across temperatures. Regarding replicate populations, the individuals used in these assays were drawn from across the six replicate populations per treatment, with each biological replicate (n = 6, with 20 individuals per replicate) comprising individuals pooled from across the replicate populations to account for inter-population variation. We have clarified this in the revised figure legend.

> *(42b) Figure 1B, Figure 5D, Figure 7: bar graphs are used for count data, so do the data represent the number of individuals with a certain trait value? If they are instead showing the mean of the population/treatment group, please use mean points ± standard errors instead.*

Accepted. The data in these figures represent continuous physiological traits (e.g., supercooling/freezing points) showing the mean of the populations, rather than count data. To align with current data visualization standards for continuous variables and to provide full transparency of the underlying data distribution, we have replaced the bar graphs in Figures 1B, 5D, and 7 with scatter plots. These revised figures now display the mean ± SEM overlaid with all individual biological replicate data points.

> *(43c) Figure 3B: There is a typo in the graph, it reads 'Stattistics' instead of 'Statistics'.*

Corrected. The typo ‘Stattistics’ in Figure 3B has been fixed.

> *(44d) Figure 3C: I don't understand what the colors of the graph mean here. Is it the average differential expression of each replicate compared to the ancestral?*

Clarified. We have updated the figure legend to explain that the colors represent the Pearson correlation coefficient (*r*) between pairs of biological replicates, indicating the degree of transcriptomic similarity among samples.

> *Methods*
>
> *(45a) Please start each new methods paragraph with the purpose of the method/analysis, for example, "To investigate XX, we used method X to measure X". It is at the moment hard to understand why certain things were done.*

We agree. We have revised each Methods paragraph to begin with a clear statement of purpose, so that the rationale for each analysis is immediately apparent. All changes are

shown in the revised manuscript.

> *(46b) Line 575-578: Why were the selection regimes with cycling temperatures and the control with constant?*

The cycling temperatures in the hot (32°C/27°C) and cold (15°C/10°C) regimes were designed to simulate diurnal temperature fluctuations (12h light/12h dark) that more closely reflect natural thermal environments. The control was maintained at a constant 26°C, which is the established optimal developmental temperature for *P. xylostella* (Liu et al., 2002) and represents the standard laboratory rearing condition. We acknowledge this asymmetry and have added a justification in the revised manuscript.

> *(47c) Line 581: How many generations was the ancestral population kept in the lab before the start of the selection experiment? And for how many generations were the populations selected?*

The ancestral population was maintained in the laboratory for approximately ~170 generations (from July 2012 to the start of the selection experiment) before the thermal selection began. The hot strain was selected for ~75 generations and the cold strain for ~15 generations over the three-year experiment. We have added this information to the revised manuscript.

> *(48d) Line 585-586: I don't understand what you mean by randomly selecting six replicate populations per treatment for downstream experiments when you only had six replicate populations per treatment to begin with (as detailed in Line 574)?*

We apologize for the confusion. All six replicate populations per treatment were used for downstream experiments. We have corrected this sentence to remove the misleading “randomly selected” wording.

> *(49e) Line 590: Were these 90 eggs also randomly selected, like for the individual life tables? And were these kept at the baseline temperature conditions?*

Yes, the 90 eggs were randomly selected and maintained under the baseline favorable temperature (26°C). We have clarified this in the revised manuscript.

> *(50f) Line 606: Which life history and population fitness parameters were calculated?*

We have specified all parameters calculated in the revised manuscript.

> *(51g) Line 609: Link to software doesn't work.*

We have updated the software link to the current working URL.

> *(52h) Line 611: Please spell out what 'BT' stands for.*

Done. “BT” has been spelled out as “bootstrap” upon first use.

> *(53i) Line 612-613: How many tests did you do? Did you correct for multiple testing? Using what method?*

The paired bootstrap method implemented in TWOSEX-MSChart inherently accounts for multiple pairwise comparisons through 100,000 bootstrap replications. We have clarified the scope of comparisons in the revised manuscript.

> *(54j) Line 620-621: What does biological replicate mean here? Individual eggs / larvae / pupae / adults, or were all or some life stages pooled? Also, you now only detailed which samples were collected for metabolomic profiling, were the same samples used for transcriptomic profiling, or a subset?*

Each biological replicate consisted of pooled individuals at the same developmental stage. The same sample collection strategy was used for both metabolomic and transcriptomic profiling, but from independent biological replicates (six for metabolomics, three for transcriptomics). We have clarified this in the revised manuscript.

> *(55k) Line 637: Also here, how many tests did you do? Were p-values corrected for multiple testing? Using what method?*

Differential metabolites were identified through pairwise comparisons using Student's t-test with FDR correction for multiple testing. A multi-criteria threshold of $|\log_2\text{Fold Change}| \geq 1$, VIP ≥ 1, and FDR < 0.05 was applied. This approach was used for all metabolomic comparisons, including HS vs. AS, CS vs. AS, and SODC-MU vs. AS. We have clarified this in the revised manuscript.

> *(56l) Line 662: And here: how many tests did you do? Did you correct for multiple testing? Using what method?*

In the WGCNA analysis, Pearson correlations were calculated between each module eigengene and each of the 30 common differential metabolites, resulting in a total of 29 × 30 = 870 correlation tests. Following standard WGCNA practice, rather than applying FDR correction, we used a stringent dual threshold of |correlation coefficient| > 0.8 and $P < 0.05$ to identify significant module-metabolite associations, which effectively controls for false positives (Langfelder and Horvath, 2008). We have clarified this in the revised manuscript.

> *(57m) Line 663: How did you select these modules? The ones that significantly correlated with differential metabolites? Why did you not use the phenotype data here?*

Modules were selected based on significant correlations (|correlation coefficient| > 0.8, $P < 0.05$) with differential metabolites shared between the hot and cold strains. We chose metabolites rather than phenotype data as the trait input for WGCNA because metabolites serve as intermediate molecular phenotypes that bridge gene expression and organismal phenotypes, providing a more direct link to the underlying regulatory mechanisms. This approach allowed us to identify gene modules most closely associated with the metabolic changes driven by thermal adaptation, which could then be connected to the observed life history and fitness divergence.

> *(58n) Line 666: move RNA extraction details to before RNAseq methods description.*

Done. The “RNA extraction and cDNA synthesis” section has been relocated to before the “Transcriptomic profiling” section for better logical flow.

> *(59o) Line 836: This paragraph describing the statistics is very short, and it is unclear to what data the described analyses apply. As the different types of data are very different, I expect the analyses to differ as well. Please describe the statistical analyses for each data type in more detail, specifying what tests you used, which, and how many comparisons were performed.*

We agree. The statistical methods for life table analysis, metabolomics, and transcriptomics have been detailed in their respective method sections. We have expanded the Data analysis section to specify the statistical tests for the remaining experimental data.

> *(60p) Line 837: Please include your SPSS scripts to ensure the reproducibility of your results.*

The statistical analyses in SPSS were performed using the graphical user interface. As all statistical tests, parameters, and comparison groups have been described in detail in the revised Methods section, and the raw data have been deposited in public repositories (see

Data availability), we believe the analyses are fully reproducible. We are happy to provide additional details if needed.

https://doi.org/10.7554/eLife.110352.2.sa0